AD-A125 072 HYDRODYNAMIC LOADING ON ARMORED TOWCABLES(U) DAVID W 1/1
TAYLOR NAVAL SHIP RESEARCH AND DEVELOPMENT CENTER
BETHESDA MD R FOLB ET AL. FEB 83 DTNSRDC-82/116

UNCLASSIFIED F/G 13/5 NL

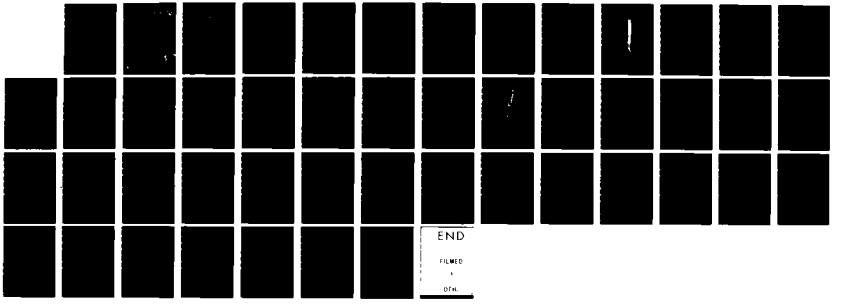

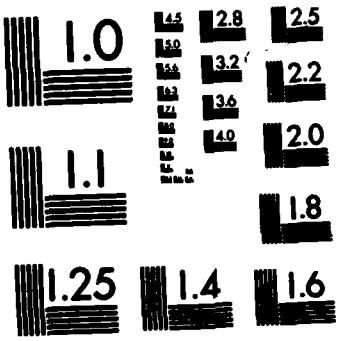

DAVID W. TAYLOR NAVAL SHIP RESEARCH AND DEVELOPMENT CENTER

Bethesda, Maryland 20084

HYDRODYNAMIC LOADING ON ARMORED TOWCABLES

by

[redacted]

APPROVED FOR PUBLIC RELEASE: DISTRIBUTION UNLIMITED

SHIP PERFORMANCE DEPARTMENT
RESEARCH AND DEVELOPMENT REPORT

February 1983

DTNSRDC-82/116

[redacted]

[redacted]

[redacted]

UNCLASSIFIED

SECURITY CLASSIFICATION OF THIS PAGE *(When Data Entered)*

REPORT DOCUMENTATION PAGE		READ INSTRUCTIONS BEFORE COMPLETING FORM
1. REPORT NUMBER DTNSRDC-82/116	2. GOVT ACCESSION NO.	3. RECIPIENT'S CATALOG NUMBER
4. TITLE *(and Subtitle)* HYDRODYNAMIC LOADING ON ARMORED TOWCABLES		5. TYPE OF REPORT & PERIOD COVERED Final 6. PERFORMING ORG. REPORT NUMBER
7. AUTHOR(s) Reece Folb John J. Nelligan		8. CONTRACT OR GRANT NUMBER(s)
9. PERFORMING ORGANIZATION NAME AND ADDRESS David W. Taylor Naval Ship Research and Development Center Bethesda, Maryland 20084		10. PROGRAM ELEMENT, PROJECT, TASK AREA & WORK UNIT NUMBERS (See reverse side)
11. CONTROLLING OFFICE NAME AND ADDRESS Naval Sea Systems Command Washington, D.C. 20362		12. REPORT DATE February 1983 13. NUMBER OF PAGES 45
14. MONITORING AGENCY NAME & ADDRESS*(if different from Controlling Office)*		15. SECURITY CLASS. *(of this report)* UNCLASSIFIED 15a. DECLASSIFICATION/DOWNGRADING SCHEDULE

16. DISTRIBUTION STATEMENT *(of this Report)*

APPROVED FOR PUBLIC RELEASE: DISTRIBUTION UNLIMITED

17. DISTRIBUTION STATEMENT *(of the abstract entered in Block 20, if different from Report)*

18. SUPPLEMENTARY NOTES

19. KEY WORDS *(Continue on reverse side if necessary and identify by block number)*

Armored Towcables
Hydrodynamic Loading of Towcables
Towcable Towing

20. ABSTRACT *(Continue on reverse side if necessary and identify by block number)*

A new set of hydrodynamic loading functions has been derived for bare armored towcable. These provide good first order engineering estimates for two-dimensional towing configurations over a wide range of cable angles, i.e. for critical-angle tows and body-dominated tows. It was found that a constant value of the normal drag coefficient (C_R=1.5), independent of Reynolds number, provides a good fit to the

(Continued on reverse side)

Csubk=1.5

DD FORM 1 JAN 73 1473 EDITION OF 1 NOV 65 IS OBSOLETE

UNCLASSIFIED

SECURITY CLASSIFICATION OF THIS PAGE *(When Data Entered)*

(Block 10)

Program Element 62543N
Task Area SF43-400-001
Work Unit 1507-101
MAR Associates, Inc. Contract N00600-79-D-2507

(Block 20 continued)

measured data when used with these loading functions. Where the hydrodynamic loading on the cable must be known very accurately, however, the particular cable must be tested.

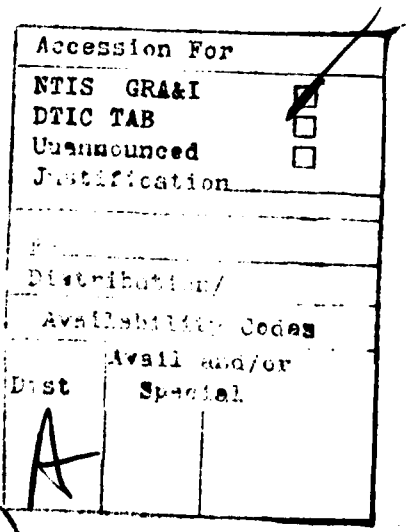

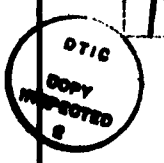

TABLE OF CONTENTS

LIST OF FIGURES

NOTATION

a	Amplitude of Vibration
A_n, B_n	Coefficients for Trigonometric Series
b	Peak-to-valley Distance on Surface of Armored Cable
C_f	Tangential Coefficient of Drag Based on Wetted Surface for Velocity Parallel to Cable Axis ($F/\frac{1}{2}\rho V^2 d\pi$)
C_R	Normal Coefficient of Drag with the Velocity 90^o to the Cable Axis ($R/\frac{1}{2}\rho V^2 d$)
C_t	Tangential Coefficient of Drag Based on Wetted Surface ($F/\frac{1}{2}\rho V^2 \cos^2\phi d\pi$)
d	Cable Diameter
f	Pode's Tangential Loading Function
f_s	Frequency of Vortex Shedding
$f_n(\phi)$	Normal Hydrodynamic Loading Function
$f_t(\phi)$	Tangential Hydrodynamic Loading Function
F	Tangential Hydrodynamic Force per Unit Length of Cable
G	Normal Hydrodynamic Force per Unit Length of Cable
$P(\phi)$	Tangential Force per Unit Length of Cable
$Q(\phi)$	Normal Force per Unit Length of Cable
R	Normal Hydrodynamic Force per Unit Length of Cable when the Velocity is 90^o to the Cable Axis
R_n	Reynolds Number (Vd/ν)
s	Cable Scope
T	Cable Tension
V	Velocity
w	Cable Weight per Unit Length in Water
λ	Cable Roughness Parameter ($2b/d$)
ν	Kinematic Viscosity
ρ	Density of Water
ϕ	Cable Angle Relative to Horizontal
ϕ_c	Critical Cable Angle
ψ	Kite Angle

ABSTRACT

A new set of hydrodynamic loading functions has been derived for bare armored towcable. These provide good first order engineering estimates for two-dimensional towing configurations over a wide range of cable angles, i.e. for critical-angle tows and body-dominated tows. It was found that a constant value of the normal drag coefficient (C_R=1.5), independent of Reynolds number, provides a good fit to the measured data when used with these loading functions. Where the hydrodynamic loading on the cable must be known very accurately, however, the particular cable must be tested.

CsubR=1.5

ADMINISTRATIVE INFORMATION

The work described in this report was performed in support of a number of projects sponsored by the Naval Sea Systems Command, the Naval Ship Engineering Center and the Naval Air Systems Command. The effort was carried out jointly by the David W. Taylor Naval Ship Research and Development Center under Program Element 62543N, Task Area SF43-400-001, Work Unit 1507-101 and MAR Associates, Inc. under DTNSRDC Contract N00600-79-D-2507. Mr. J. Nelligan is with MAR Associates, Inc. of Rockville, Maryland.

INTRODUCTION

For many years mathematical models have been available for computing the two-dimensional towing configuration of a cable under steady-state conditions. The differential equations describing towcable geometry as a function of the steady forces acting appear in Pode[1*] among other sources. For armored cables the concept of a two-dimensional steady-state configuration is somewhat idealized. The cable under tension is an elastic structure which when oriented at an angle to the flow resonates (strums) in response to vortex shedding. The attendant hydrodynamic forces are oscillatory, or have oscillatory components. Also when the armored cable's helical outer wrap of wires (Figure 1) is exposed to the flow an asymmetric flow is induced, from which results a lateral force and towcable kiting. As a consequence the cable does not lie in the plane of the free stream velocity and gravity vectors; therefore, the problem is not strictly two-dimensional.

---

*A complete listing of references is given on page 35.

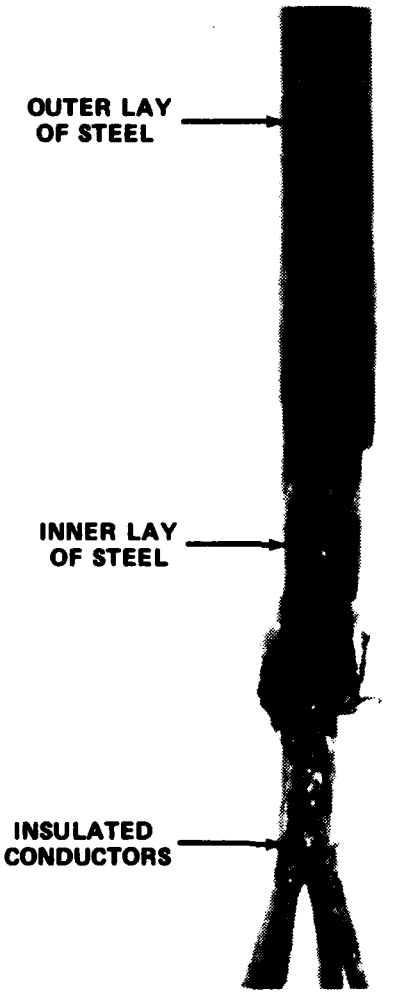

Figure 1 - Typical Armored Towcable

Nonetheless the concept of a steady-state two-dimensional configuration is useful in addressing many engineering problems, and hence it will be retained.

The key to configuration prediction lies in the ability to define the forces acting on the cable, specifically the hydrodynamic forces. Although round cables have been towed for many years, a knowledge of these forces has been difficult to acquire because of the problem of modelling long flexible (strumming) cables in either wind tunnels or towing basins. Since the round cable has a superficial resemblance to a circular cylinder, the large base of theoretical and experimental data available on cylinders has served to provide the initial guidance in formulating cable hydrodynamic loading. However, as more measurements were made on towed systems at sea significant discrepancies between prediction and measurement were noted. As a result, in the early 1960's DTNSRDC designed an at-sea experiment to determine hydrodynamic loading functions from measurements on body-dominated, armored cable towing configurations.[2] This experiment confirmed Pode's assumptions regarding loading function form and the normal drag coefficient value of 1.5 for relatively short cable, body-dominated configurations.

More recently Navy system developments in towed sonar arrays and submarine communications buoy systems have involved configurations where significant portions of the towcable were at very shallow angles. Here again a trend was found which tended to overpredict both the vertical separation and cable tension. Consequently a series of experiments was conducted on long armored cables towed at their critical angles. The analyses of these results produced a wide range of drag coefficients along with variations in the loading functions. The situation which exists today is one where the system designer is confronted with this wide range of drag coefficients and loading functions, each of which has been derived from a particular size of armored cable operating over a restricted range of towing angles.

The purpose of this investigation is to establish a set of hydrodynamic loading functions which will reasonably predict armored towcable configurations for both body-dominated tows and critical-angle tows. The report contains a discussion of the hydrodynamic forces on armored cable and how they are represented for the purpose of computing towing configurations. A number of data bases is then employed in developing the hydrodynamic loading functions. Finally a comparison of predicted-to-measured towing configurations is presented to show the degree of agreement provided by a single set of loading functions.

BASIC CONSIDERATIONS

The differential equations describing the steady-state configuration of a cable in a uniform stream require as inputs expressions for the forces acting on the cable. For the two-dimensional case the usual practice has been to assume the armored cable lies in the velocity/gravity plane and to resolve the loading into force components normal and tangential to the cable's longitudinal axis. Also the usual practice has been to express these components as functions of the cable's angle of inclination ϕ relative to the horizontal. The equations describing the force balance normal and tangential to the cable as depicted in Figure 2 can be expressed:

$$\begin{aligned} Td\phi &= -Q(\phi)ds \\ dT &= -P(\phi)ds \end{aligned} \qquad (1)$$

where

$$\begin{aligned} Q(\phi) &= G - w\cos\phi \\ P(\phi) &= -(F + w\sin\phi) \end{aligned} \qquad (2)$$

and where G and F are the normal and tangential components of hydrodynamic force per unit length of cable, respectively, and w is the cable weight per unit length in water.

From engineering practice has evolved the form of the expressions used for the normal, G, and tangential, F, components of hydrodynamic force per unit length of cable. The usual forms are:

$$\begin{aligned} G &= f_n(\phi)R \\ F &= f_t(\phi)R \end{aligned} \qquad (3)$$

In this formulation the terms $f_n(\phi)$ and $f_t(\phi)$ are assumed to depend totally on the inclination angle. R is defined as follows:

$$R = \tfrac{1}{2}\rho C_R V^2 d \qquad (4)$$

where

ρ = the density of water,

C_R = the normal drag coefficient for flow 90^o to the cable axis,

V = velocity, and

d = cable diameter.

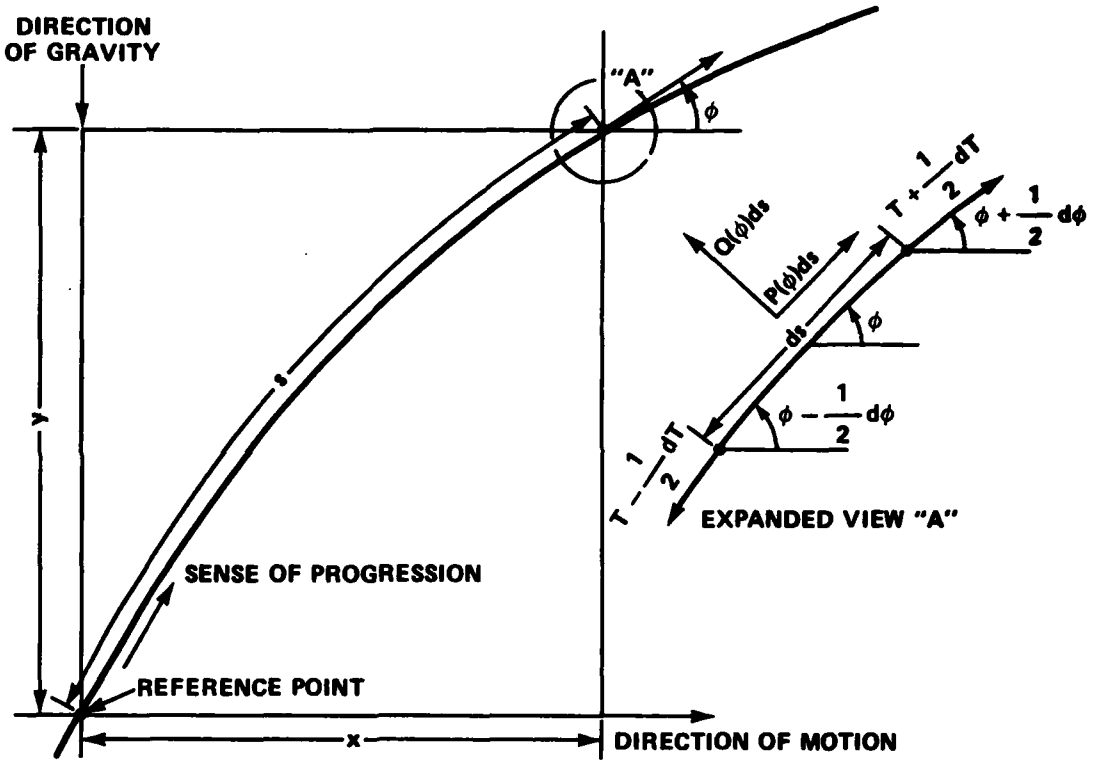

Figure 2 - Coordinate System and Forces on an Incremental Length of Cable

Certain problems arise with this particular formulation of the hydrodynamic loading functions. The first involves the use of C_R to scale both the normal and tangential force components. Although there is evidence of a physical relationship between C_R and G, it is difficult to rationalize one between C_R and F. If Reynolds' number R_n effects exist, then C_R is the parameter by which these effects are properly accounted for. Yet R_n effects on drag for flow normal to a cable would seem to be unrelated to those for tangential flow in the R_n range of most practical interest to towing problems; i.e. from 10^4 to 3×10^5.

Therefore, to the extent that:

1. there are R_n effects on the normal or tangential force components, and
2. these effects differ,

then by forcing C_R to account for all R_n effects (Equation (3)) in the process of deriving C_R from measured data:

1. there must be a compromise in which neither of the derived functions F and G represent the actual forces as well as they might, i.e. if both were not forced to be scaled by C_R, or
2. certain of the R_n effects become improperly assigned to the $f_n(\phi)$ and $f_t(\phi)$ functions.

A second problem which arises in relating the hydrodynamic loading to C_R is that C_R is difficult to measure directly for a round towcable. The resonant vibration patterns which develop in a long heavy towcable are difficult to achieve in either a wind tunnel or a towing basin. As a result, C_R is a derived coefficient, one determined from measurements on long cables towed at angles other than 90^o (to the flow) by a procedure which requires first assuming forms for the hydrodynamic loading functions. Depending on the forms assumed for $f_n(\phi)$ and $f_t(\phi)$, C_R can attain that range of values needed to match F and G to the measured data. If these data are concentrated around the shallow angles, as is usually the case, then the permissible ranges of $f_n(\phi)$ and $f_t(\phi)$ are especially large and the potential range for C_R is also large. Consequently, C_R as derived in practice is not "the characteristic" drag coefficient dependent only on R_n but is a coefficient (one in a range of values) linked to the particular loading functions by which it was derived.

NORMAL HYDRODYNAMIC FORCE

An important factor in the normal component of hydrodynamic force is cable strumming. It is induced by vortex shedding from a round cable under tension and inclined at an angle to the flow. Strumming is a resonant vibration; it produces a lateral standing wave and is characterized by synchronization of the flow field and vibrating cable. The hydrodynamic force, therefore, has oscillatory components which may be resolved normal and tangential to the cable in the plane of tow and lateral (or perpendicular) to the plane of tow. The fluid force supporting strumming is the lateral hydrodynamic force component which both supplies energy (lift) to and extracts energy (damping) from the vibrating cable. This lateral fluid force is coherent over a half wave length of cable scope and oscillates at the vortex shedding frequency

$$f_s = \frac{0.2\ V \sin\phi}{d} \qquad (5)$$

This is the Strouhal frequency provided $10^3 < R_n < 10^5$.

Vortex shedding also affects the fluid force in the plane of tow. Onto the large steady component of the normal fluid force there is superimposed an oscillatory component[3] at a frequency $2f_s$. For the strumming cable at 90^o to the flow the total hydrodynamic force in the plane of tow is, by definition, $G = R$. As the cable is then inclined in the plane of tow the normal component of hydrodynamic force has been observed to be a function of the cross-flow component of velocity, or $G \propto \sin^2\phi$. This relationship has been demonstrated to hold over a wide range of inclination angles (although not at shallow angles) for experiments on cylinders[4] and on short-length cable models.[5]

As noted earlier, obtaining R (or C_R) by direct measurement is very difficult for real cables because of the problems associated with modelling a strumming cable in the restricted depth of a model basin or water tunnel. The literature on circular cylinders provides some guidance, however. The effect of resonant vibration on C_R for an oscillating circular cylinder can be seen in Figure 3. Data points[3,6,7] refer to cylinders forced to vibrate at the Strouhal frequency for a range of amplitude ratios $\frac{a}{d}$. Near $R_n = 10^4$ the vibrations produce high values of C_R; at least twice that for a stationary cylinder. As R_n increases, apparently there is a transition and C_R falls as would be expected for a stationary cylinder. To place these cylinder data in context, the maximum amplitude ratio for a strumming cable

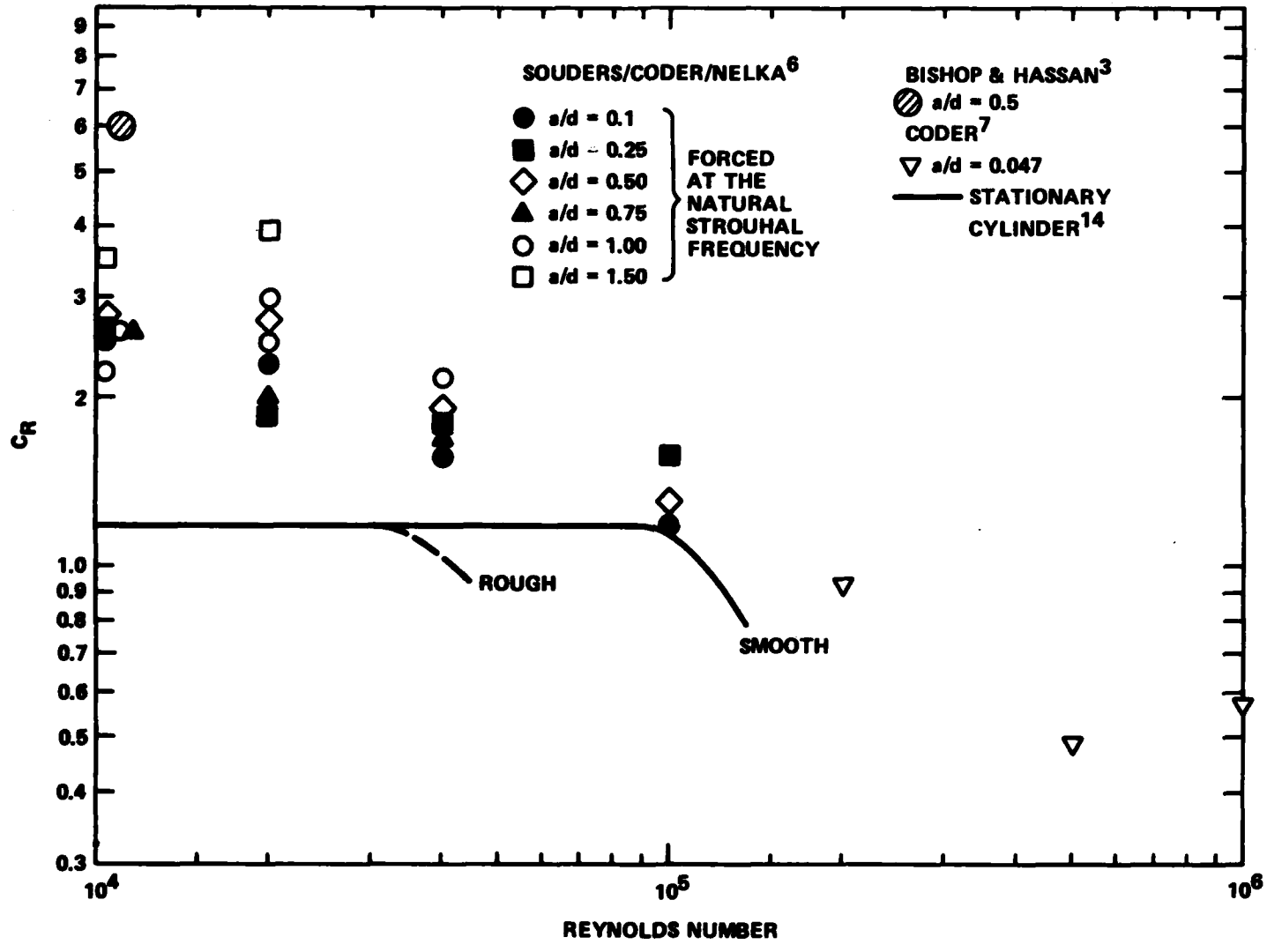

Figure 3 - Effect of Vibration at the Strouhal Frequency on C_R for Cylinders

is estimated[8] to be 1.2. Unfortunately, however, even though the data point to a trend of higher C_R with vibration the magnitudes shown in Figure 3 for cylinders are not directly applicable to resonating cables.

Some characteristics of cable strumming in actual towing configurations should be mentioned because of potential effects on the hydrodynamic normal force. First, with respect to strumming frequency, in a critical angle tow the frequency is expected to be constant along the entire scope, neglecting end effects (low tension) at the outboard end. This frequency is virtually unvarying with speed as the product $V\sin\phi$ changes little with speed over a broad speed range. For a body-dominated tow the cable inclination angle varies continuously along the scope and vortex shedding frequency will be higher near the body (i.e. at the steeper angles) and lower near the ships' towpoint. In both cases tension varies along the cable. The effects of these variations on strumming intensity and normal hydrodynamic force are not known.

Even though C_R has not been measured directly, it is possible to derive $G(\phi)$, the normal component of hydrodynamic force on the strumming cable at inclination angles less than 90°. By applying Equations (2), (3) and (4) using a regression analysis a normal hydrodynamic loading function and a value of C_R can be derived jointly. This has been done in a number of experiments[2,9,10]; the results are listed in Table 1.

TABLE 1 - EXPERIMENTALLY DERIVED VALUES OF C_R

Experiment	Cable Size	Cable Angle Range	Normal Hydrodynamic Loading Function	C_R
Reference 9	0.322 in. (0.82 cm)	0.6° - 10.5°	$\sum_{n=1}^{10} A_n \sin(2n-1)\phi$	1.1294
Reference 9	0.542 in. (1.38 cm)	4° - 12°	$\sum_{n=1}^{10} B_n \sin(2n-1)\phi$	1.1294
Reference 2	0.35 in. (0.89 cm)	8° - 85°	$\sin^2\phi$	1.5
Reference 10	0.84 in. (2.13 cm)	5° - 15°	$f(\phi/\psi)\sin^2\phi$	1.0-2.0*

*Technically Reference 10 treated kiting of the towcable and derived a normal force coefficient $C_N \neq C_R$. However, the difference becomes significant only for very small ϕ.

One possible cause of the differences in the derived C_R's in Table 1 is the difference in the assumed value of $f_n(\phi)$, an issue which was discussed previously. As to whether Reynolds number effects are involved, neither the work in Reference 2 nor 9 found any R_n effect on C_R. The R_n range covered by certain critical angle towing experiments is indicated in Figure 4.

TANGENTIAL HYDRODYNAMIC FORCE

For heavy cables the tangential hydrodynamic force and the cable's weight act to produce the incremental buildup of tension in the towcable. The tangential hydrodynamic force should be discussed in relation to the two basic types of towing configurations; body-dominated tows in which the cable angle is continuously changing over the major part of the scope and critical-angle tows in which there is no (or very little) change in angle over the length of towcable. In a body-dominated tow the tangential hydrodynamic force on the bare towcable is typically small compared to the other forces acting. As a result:

1. in most body-dominated tows the accurate prediction of the tangential component of hydrodynamic force is not a critical requirement,
2. but, for the same reason, measuring this force accurately is difficult.

Therefore for body-dominated tows the simple, though physically implausible, formulation by Pode[1] wherein the tangential hydrodynamic loading is treated as a constant independent of angle has proven to be an adequate predictive model.

However, systems using long towcables at high speed (critical-angle tows) are becoming more important to the Navy (e.g. towed arrays). For these tows the tangential hydrodynamic force predominates, and with safety margins usually being squeezed, its accurate prediction is most important. For such tows the Pode model was proven to be inadequate. Experiments were performed[9,10] in which long lengths of armored cable were towed at shallow critical angles and the tangential loading was measured. Some of the results have been reduced to coefficient form and plotted in Figure 5 together with some earlier measurements on stranded cable, which have essentially the same exterior structure as armored cable.

There are some differences in the methods of reduction and presentation of tangential force data. Consequently, some discussion of the tangential drag coefficient C_t in use is warranted. Another coefficient C_f based on wetted surface area

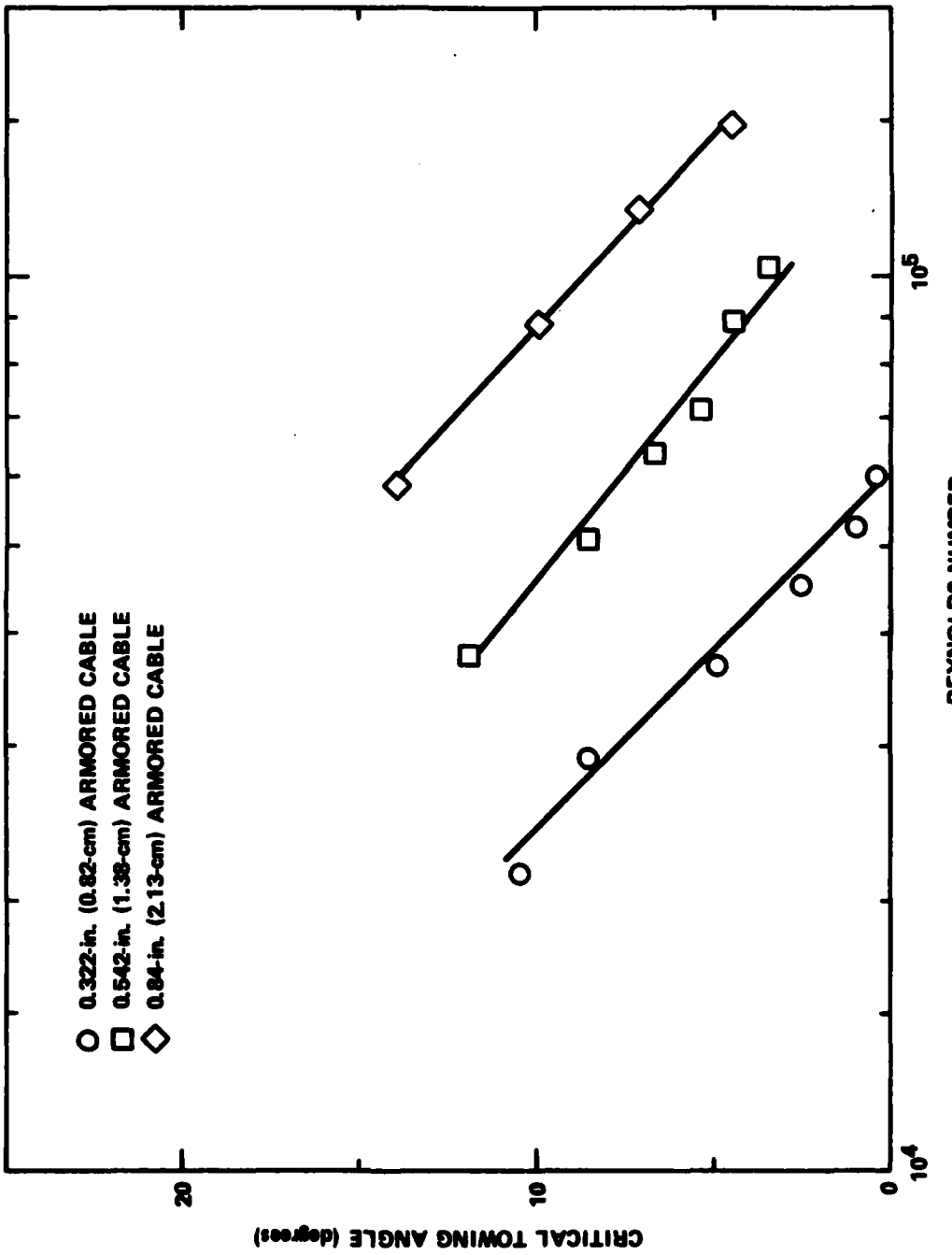

Figure 4 - Cable Angle versus Reynolds Number for Critical Angle Tows

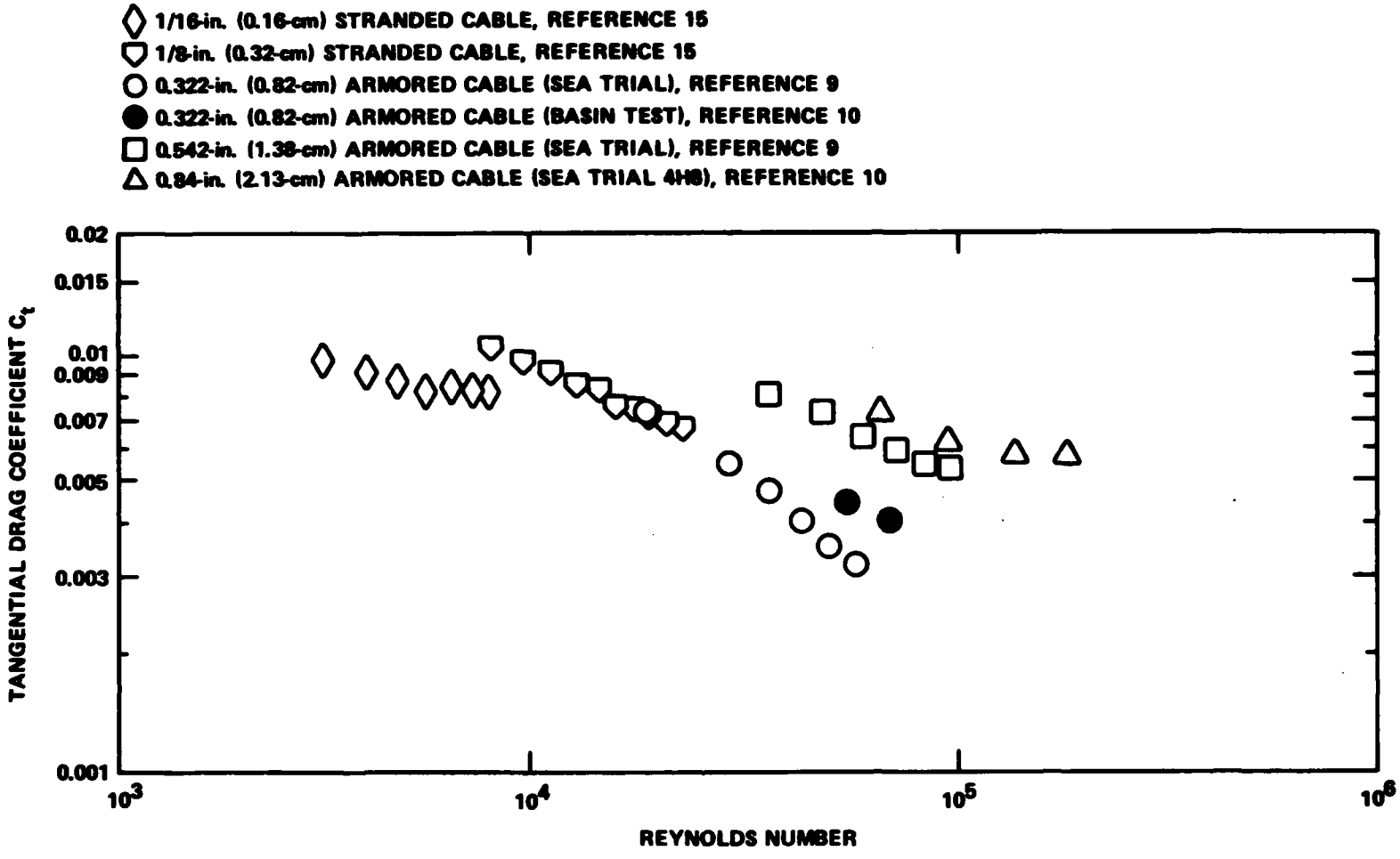

Figure 5 - Measured Tangential Drag Coefficients versus Reynolds Number

is defined here as a friction force coefficient and its use implies a free stream velocity parallel to the cable's axis. In the case of (heavy) armored cable its applicability is extremely limited, but in theory it does represent the limiting value of C_t as ϕ approaches 0^o. C_t is the more general form for C_f in that the constraint of a parallel free stream velocity is removed. Even so C_t is often referred to also as a friction force coefficient. In presenting measured force data in terms of C_t, ϕ may or may not be treated explicitly. When it is, the assumption is usually made that the tangential hydrodynamic force is a function of the tangential component of velocity or $F \propto \overline{V\cos\phi}^2$. In practice critical angle tows generally involve angles less than 15^o so that the $\cos\phi$ modification to free stream velocity is small. The drag data are usually presented in the form C_t versus Reynolds number as in Figure 5.

This representation of the data causes difficulty in its application. Figure 5 shows that both for stranded cable and armored cable there can be more than one value of C_t at a given R_n. Clearly Reynolds scaling alone does not permit measured data for one cable to be applied to a similar type cable of different diameter.

Also, shown in Figure 4, is a consistent inverse relationship between R_n and cable angle for critical angle tows. The question of which is the primary relationship $C_t = f(R_n)$ or $C_t = g(\phi)$ was addressed by Gay and Puryear in Reference 12. It was concluded that the data base of Reference 12 would not support a resolution of this question.

In a theoretical treatment of the tangential hydrodynamic force Reid and Wilson[11] developed a model of the tangential drag coefficient (for stranded cable) assuming that the force is frictional. The coefficient is a function of a roughness parameter λ, a turbulence level parameter and Reynolds number. It can be seen in Figure 6, reproduced from Reference 11, that for R_n values associated with cable towing (i.e. $R_n > 10^4$) and for roughness ranges applicable to stranded aircraft, cable ($0.2 < \lambda < 0.38$) the model predicts (solid horizontal lines) that tangential drag coefficient is a function of λ but independent of R_n. The experimental data shown in Figure 6, however, indicate a dependence of C_t on R_n.

While this model was developed with stranded cable in mind, the theory is applicable to armored cable as well. The roughness parameter λ (= 2b/d) is a measure of the peak-to-valley distance (b) seen as armor wires (or cable strands) laid side by side on the cable's circumference. For armored cable λ is in the range

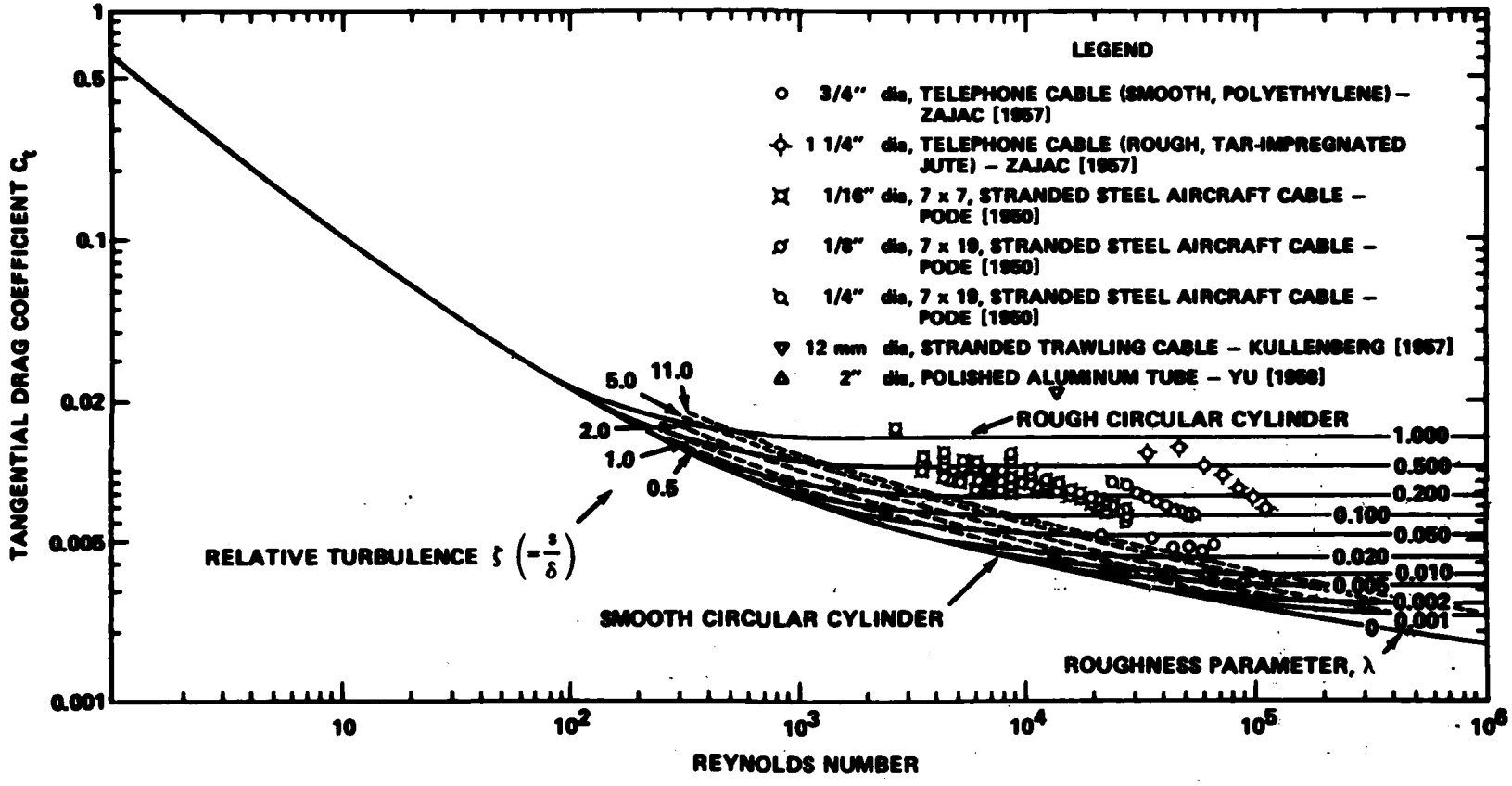

Figure 6 - Relationship of Tangential Drag Coefficient to Reynolds Number

of 0.03 to 0.12. This range of λ corresponds to a range of values of C_t from 0.0045 to 0.006 predicted from Figure 6, which falls generally in the range of data points for armored cable shown in Figure 5. This general agreement in the range of predicted and measured C_t is of little practical use, however, since the spread in measured C_t is quite large for each cable and more so across all cables, and Reynolds scaling provides no guidance in determining specific values of C_t.

The picture which emerges is one of a fundamental lack of understanding of the nature of the tangential hydrodynamic force. From this we find in practice a lack of precision and clarity in the presentation and use of measured data. It is not surprising then that there is a lack of agreement in formulating tangential hydrodynamic loading functions for use in towing configuration computer programs. As noted earlier, Pode[1] assumed the loading function:

$$f_t = f = F/R$$

where f is a constant dependent upon cable surface roughness but independent of ϕ across the entire range from 0^o to 90^o.

In Reference 9 a loading function was developed as a function of ϕ in which critical angle towing data were used to establish $f_t(\phi)$ at angles up to about 15^o and wind tunnel data by Relf and Powell[5] were used to define the function over the remaining angle range to 90^o. This function shows a sharp increase in value with increasing ϕ in the range of small angles, a slope sign reversed in the mid-range of ϕ and a value of zero at $\phi = 90^o$. The steep positive slope at small ϕ is difficult to explain. It seems inconsistent with the concept that the tangential hydrodynamic force is mainly frictional. It may reflect some additional drag induced by lift at the small angles, but this has never been demonstrated.

DETERMINATION OF LOADING FUNCTIONS

The data base used to determine the loading functions consists of measurements from the following two types of towing configurations;

1. the body-dominated tow (Reference 2) which involves cable angles from 9^o to 86^o but for which the data are heavily concentrated in the middle angle range, and
2. critical-angle tows (References 9 and 10) in which the data are for inclination angles of 15^o and less.

These two types of data must be treated differently in developing the new loading functions. Critical angle towing is most useful in determining the loading functions since it provides direct measurement of hydrodynamic loading on the cable. However, the disadvantages of these data in formulating loading functions are that in practice they cover only a narrow range of shallow towing angles and for a specific cable each angle implies a corresponding speed so that it is not possible to determine the effects of angle and speed independently.

The body-dominated towing data cover a broad range of angles at each speed but in practice it is very difficult to measure the hydrodynamic forces directly in such configurations. Rather the hydrodynamic loading is generally deduced by assuming forms of the loading functions until the computed and measured towing configurations (i.e. tension and depth as functions of speed and scope) agree. The loading functions are inferred from the data.

The method of developing the new loading functions reflects these limitations imposed by the character of the data bases. In the shallow angle regime, $f_n(\phi)$ and $f_t(\phi)$ are determined (for an assumed value of C_R) as a best fit to the critical angle towing measurements. The functions are defined over the remainder of the angle range by assuming $f_n(\phi)$ and $f_t(\phi)$ over this range until a satisfactory fit of computed-to-measured configurations is attained.

The normal loading function is addressed first. Data from the critical angle tows are expressed in terms of the parameter $[f_n(\phi_c) \cdot C_R]$ obtained by combining the normal components in Equations (2) and (3). For critical angle tows, since $Q = 0$,

$$[f_n(\phi_c) \cdot C_R] = \frac{w \cos\phi_c}{\frac{1}{2}\rho V^2 d} \qquad (6)$$

The parameter $[f_n(\phi_c) \cdot C_R]$ is a dimensionless measure of the unit normal hydrodynamic force. Figure 7 shows the available critical-angle towing data for armored cable evaluated in terms of this parameter. The dashed line is the Walton/Gibbons function $[f_n(\phi) \cdot C_R = 1.5 \sin^2\phi]$ extended into the shallow angle range. It can be seen that the measured data are generally higher valued than the dashed curve. The discrepancy becomes more significant as the cable angle becomes more shallow; here the average of the data points is about 100% greater than $[1.5 \sin^2\phi]$ at $\phi = 5^\circ$. This demonstrates why $\sin^2\phi$ is a poor model of the normal hydrodynamic loading function at shallow angles, since reasonable values of C_R

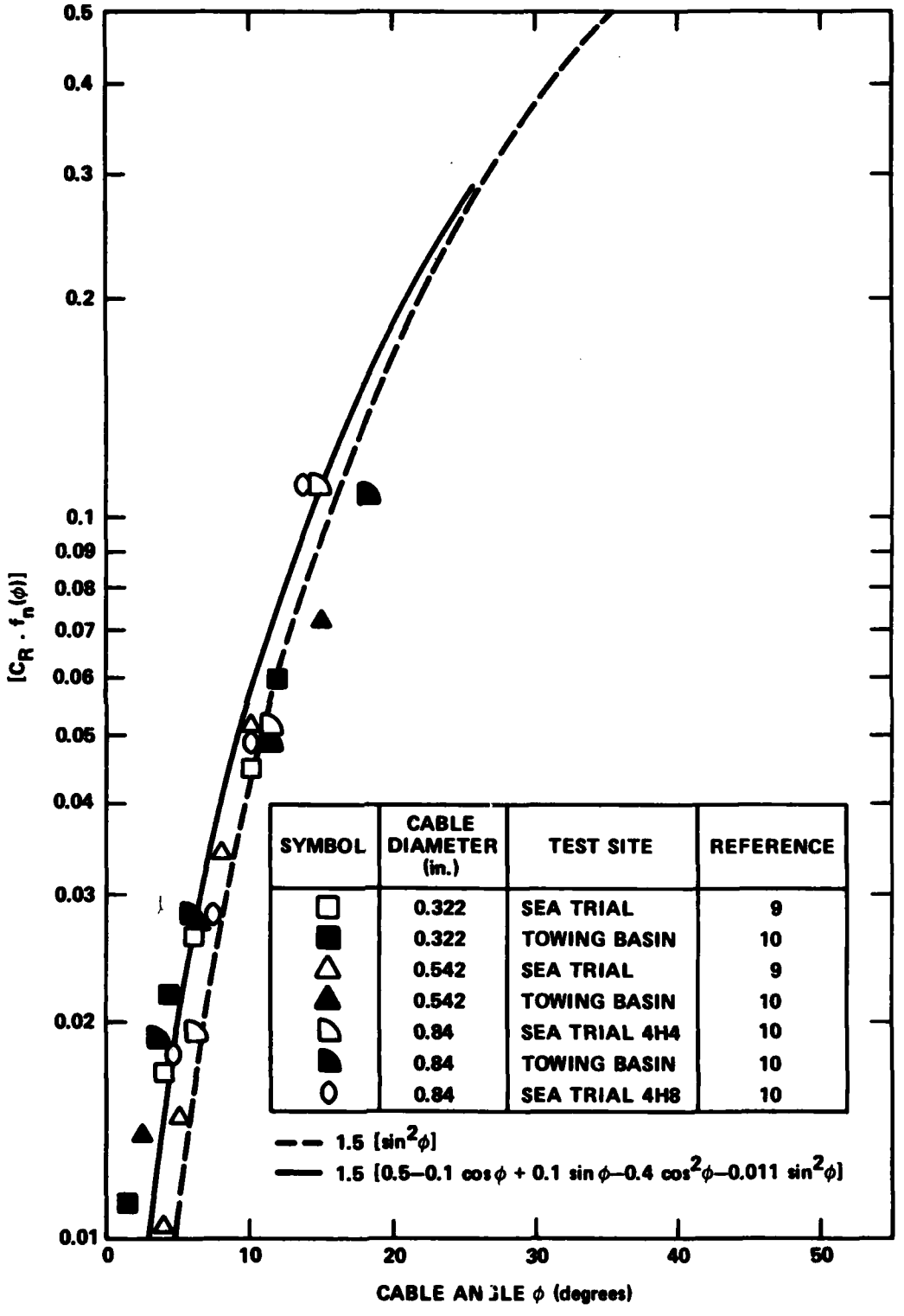

Figure 7 - Dimensionless Normal Hydrodynamic Force versus Cable Angle

would result in underprediction of the hydrodynamic normal force and overprediction of towing depth.

In deriving a new $f_n(\phi)$ function an effort was made to retain the value of $C_R = 1.5$ and the functional form of $f_n(\phi) \approx \sin^2\phi$ at mid to high values of ϕ. This was done because this model has already been shown to be a good fit to the Walton/Gibbons data. The task then became one of modifying $f_n(\phi)$ in the low angle range to provide a good fit to the critical angle towing data.

The solid line in Figure 7 represents the small angle segment of the newly derived function $f_n(\phi)$. It is expressed in terms of a truncated trigonometric series, a mathematical form which has become the standard in practice because of its compatibility with existing computer program formats; the result is:

$$f_n(\phi) = 0.5 - 0.1\cos\phi + 0.1\sin\phi - 0.4\cos2\phi - 0.011\sin2\phi, \quad (7)$$

with $C_R = 1.5$.

This function is not a least squares fit to the data. Rather, subjective judgments were made in weighting certain of the data points more heavily than others. For example, the solid data points are from experiments conducted in the DTNSRDC towing basin. The points above 10° pertain to relatively short lengths of cable where it would be expected that strumming was not fully developed because of small cable tension. These data are thus weighted less heavily. Other towing basin data, at angles less than 10°, pertain to longer lengths of cable; these are weighted more evenly with data obtained at sea.

The new function $f_n(\phi)$ is shown over the full angle range in Figure 8 as a series of computed points. The solid line represents $\sin^2\phi$; it is shown here for comparison purposes. The agreement between the two curves is close in the middle range of angles. A discrepancy is apparent in the range, $60^\circ < \phi < 80^\circ$, but the average difference is only 2.5%. The more significant difference in magnitude not apparent in Figure 8 because of the scale but evident in Figure 7 occurs at the shallow angles. Noted also in Figure 7 is the fact that even though the data points appear to fall in a reasonably narrow band there is, in fact, so much scatter that no single function $[f_n(\phi) \cdot C_R]$ can closely represent all of the data.

In developing the tangential hydrodynamic loading function $f_t(\phi)$ the critical angle data were again used to define the function in the shallow angle range. Combining Equations (2) and (3) for critical angle tows:

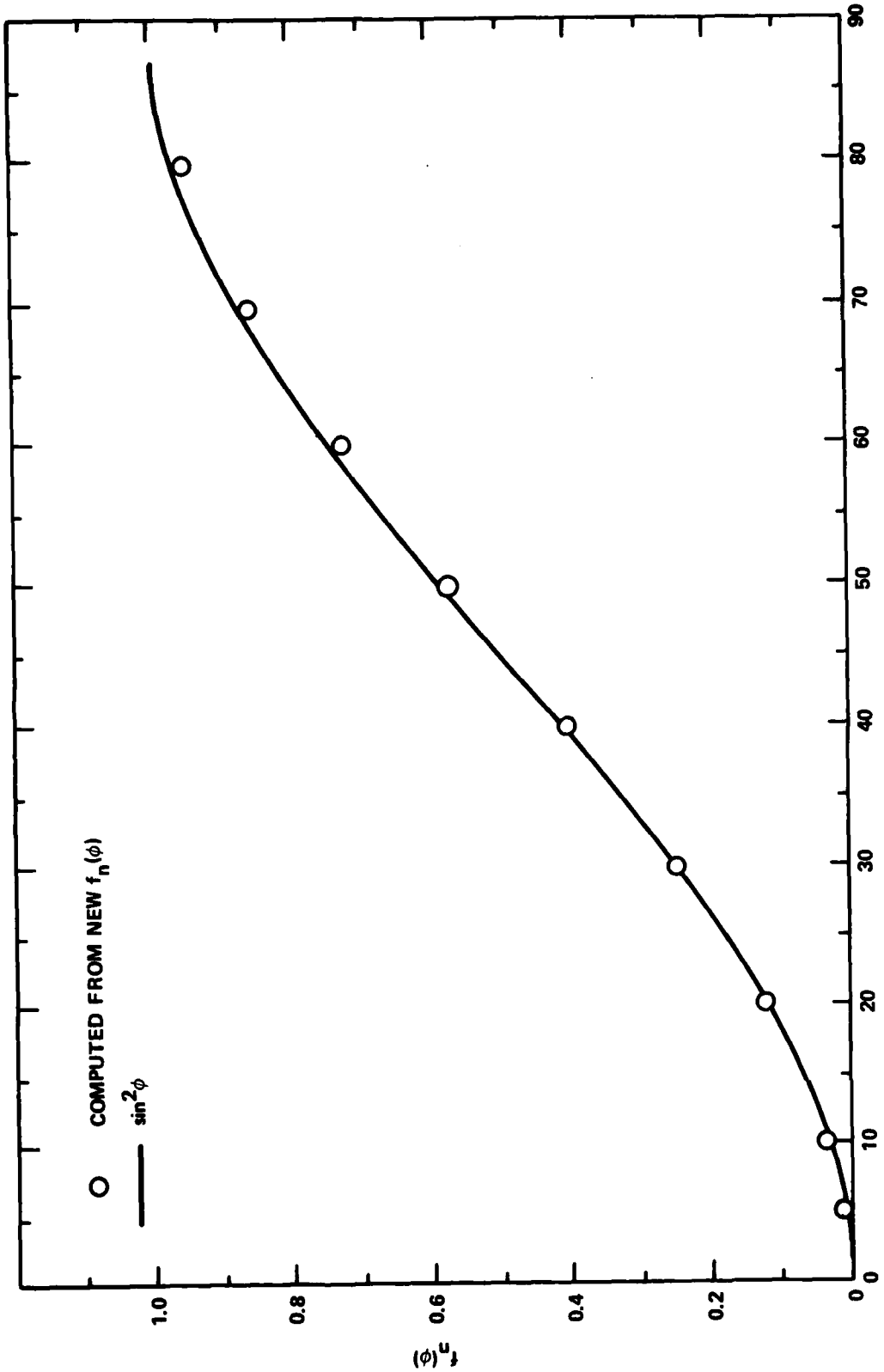

Figure 8 - New Normal Hydrodynamic Loading Function and $\sin^2\phi$ versus Cable Angle

$$\frac{dT}{dS} = -P(\phi) = F + w\sin\phi \tag{8}$$

$$f_t(\phi_c) = \frac{dT/dS - w\sin\phi_c}{\frac{1}{2}\rho C_R V^2 d} \tag{9}$$

Using the data of References 9 and 10, discrete values of $f_t(\phi)$ were computed for each speed of tow, assuming $C_R = 1.5$. These values are shown as data points in Figure 9. Except for the at-sea tests of the 0.322-inch (0.82-cm) diameter cable the data produce a rather closely defined trend of $f_t(\phi)$ with ϕ. The 0.322-inch cable (at-sea) data base raises certain questions concerning its accuracy:

1. the unusually low minimum value of the tangential drag coefficient seen in Figure 5,
2. the high value of tension at the (projected) zero scope intercept seen later in Figure 14, and
3. the disagreement between the at-sea and towing basin tangential force measurements for the 0.322-inch (0.82-cm) diameter cable seen in Figures 5 and 9.

For these reasons, and particularly since the 0.322-inch (0.82-cm) cable data points derived from basin tests are in good agreement with the trend established by all other data, the at-sea 0.322-inch (0.82-cm) cable data are given no weight in formulating the function $f_t(\phi)$.

In defining the function $f_t(\phi)$ over the entire angle range the approach taken was somewhat similar to that used in reference 9:

1. for the range of $\phi < 15^o$, the critical angle towing data are used to define the function,
2. to define the function at the higher angles a regression analysis was performed to fit the predicted towing tension to that measured in the (body-dominated) experiments of reference 2, and
3. the function was required to be zero at $\phi = 90^o$.

By trial and error the function shown as a solid line in Figure 10 was developed which produced a reasonably good fit to all the data available and could be expressed as a smooth function in terms of the truncated trigonometric series.

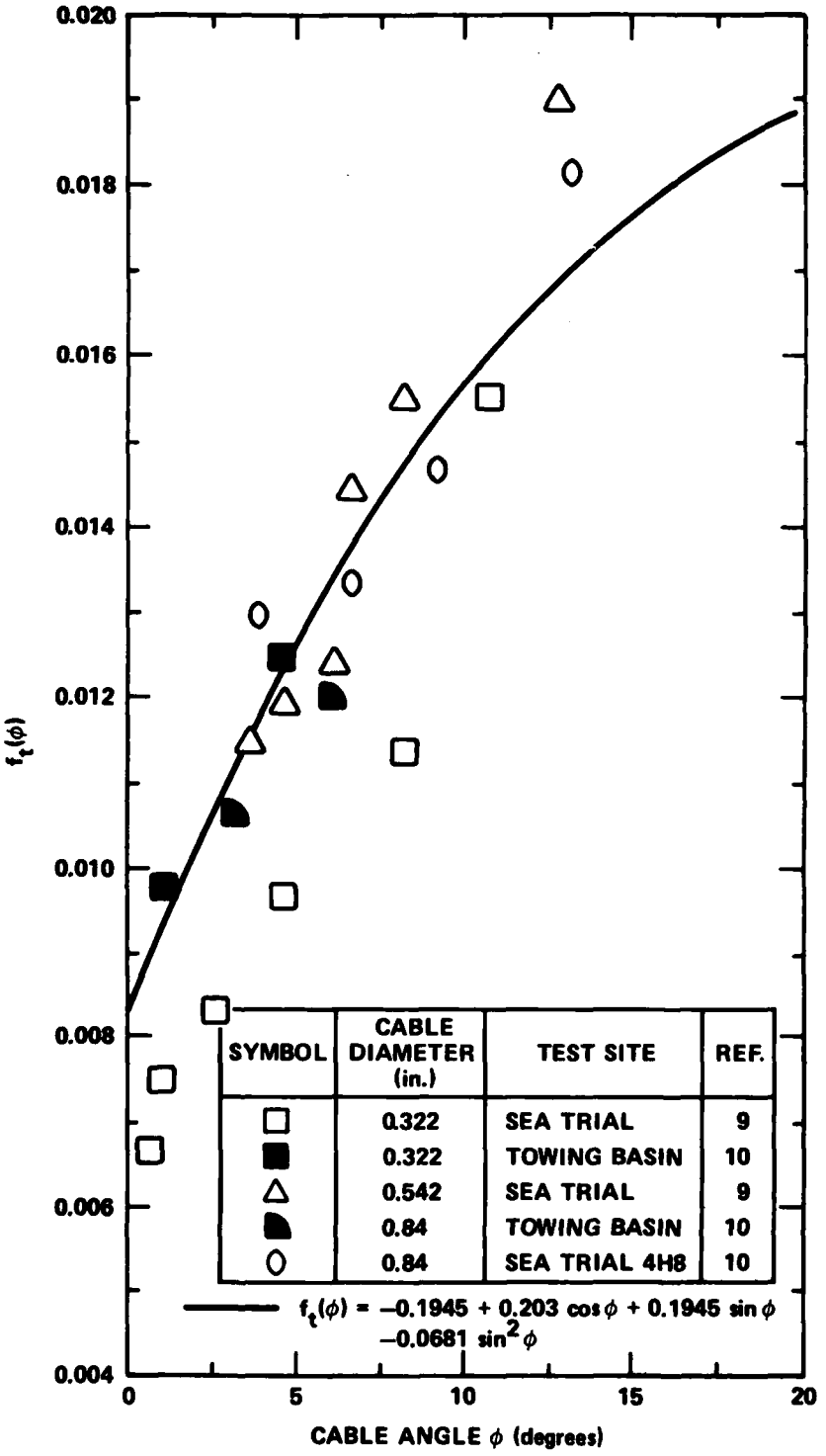

Figure 9 - Tangential Hydrodynamic Loading versus Cable Angle at Shallow Angles

The function which was developed for $C_R = 1.5$ is:

$$f_t(\phi) = -0.1945 + 0.203 \cos\phi + 0.1945 \sin\phi - 0.0681 \sin 2\phi \qquad (10)$$

It can be seen in Figure 9 that the function falls somewhat below the data points at 12.5^o. This was required to produce a smooth function in the terms of the trigonometric series which agreed with the Walton/Gibbons data. The difference between the function $f_t(\phi)$ and the average of the data points at 12.5^o is about 10%.

DISCUSSION

It is apparent from Figures 7 and 9 that there will be some discrepancy between the model predictions based on the new loading functions and each of the particular data bases from which they were derived. Therefore a comparison has been performed to gain some insight into the degree of differences to be expected. The data bases used for these comparison are:

1. critical angle tow, 0.542-inch (1.38-cm) cable, Reference 9;
2. critical angle tow, 0.322-inch (0.82-cm) cable, Reference 9;
3. critical angle tow, 0.84-inch (2.13-cm) cable, Reference 10; and
4. body-dominated tow, 0.35-inch (0.89-cm) cable, Reference 2.

Figures 11 and 12 show a comparison between the new model predictions for the depth of tow and the towpoint tension, respectively, for the 0.542-inch (1.38-cm) diameter cable and the measured data from the at-sea experiments. The solid lines represent the model predictions. It is seen that the model underpredicts depth by about 10% to 12%, i.e., it predicts a slightly shallower towing angle than measured. This is to be expected. In Figure 7 the appropriate data points are seen to fall uniformly below the new loading function $f_n(\phi)$ implying that the predicted normal hydrodynamic force will be greater than the observed in this case. With respect to towpoint tension (Figure 12) the agreement is quite good. For the 6, 10 and 16 knot cases the discrepancy between the computed points and the faired curves is less than 10%, for the most part less than 5%.

Figures 13 and 14 show a comparison of new model predictions with the measured towing depth and towpoint tension data, respectively, from at-sea measurements on the 0.322-inch (0.82-cm) cable for speeds of 6, 10 and 16 knots. As discussed previously, this data base and particularly the cable tension data has characteristics which raise doubts as to its accuracy. Nonetheless it is a published data

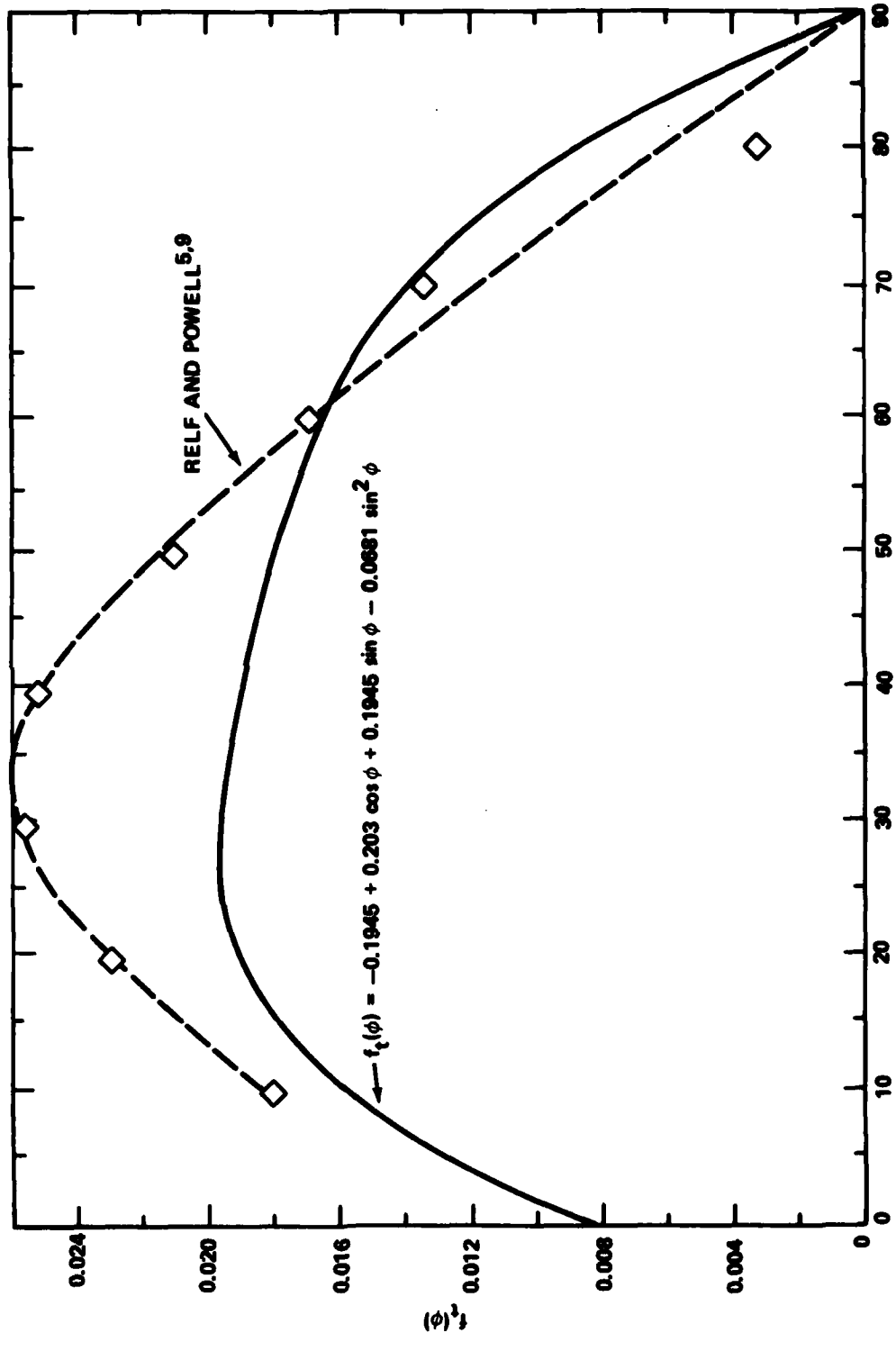

Figure 10 - New Tangential Hydrodynamic Loading Function versus Cable Angle

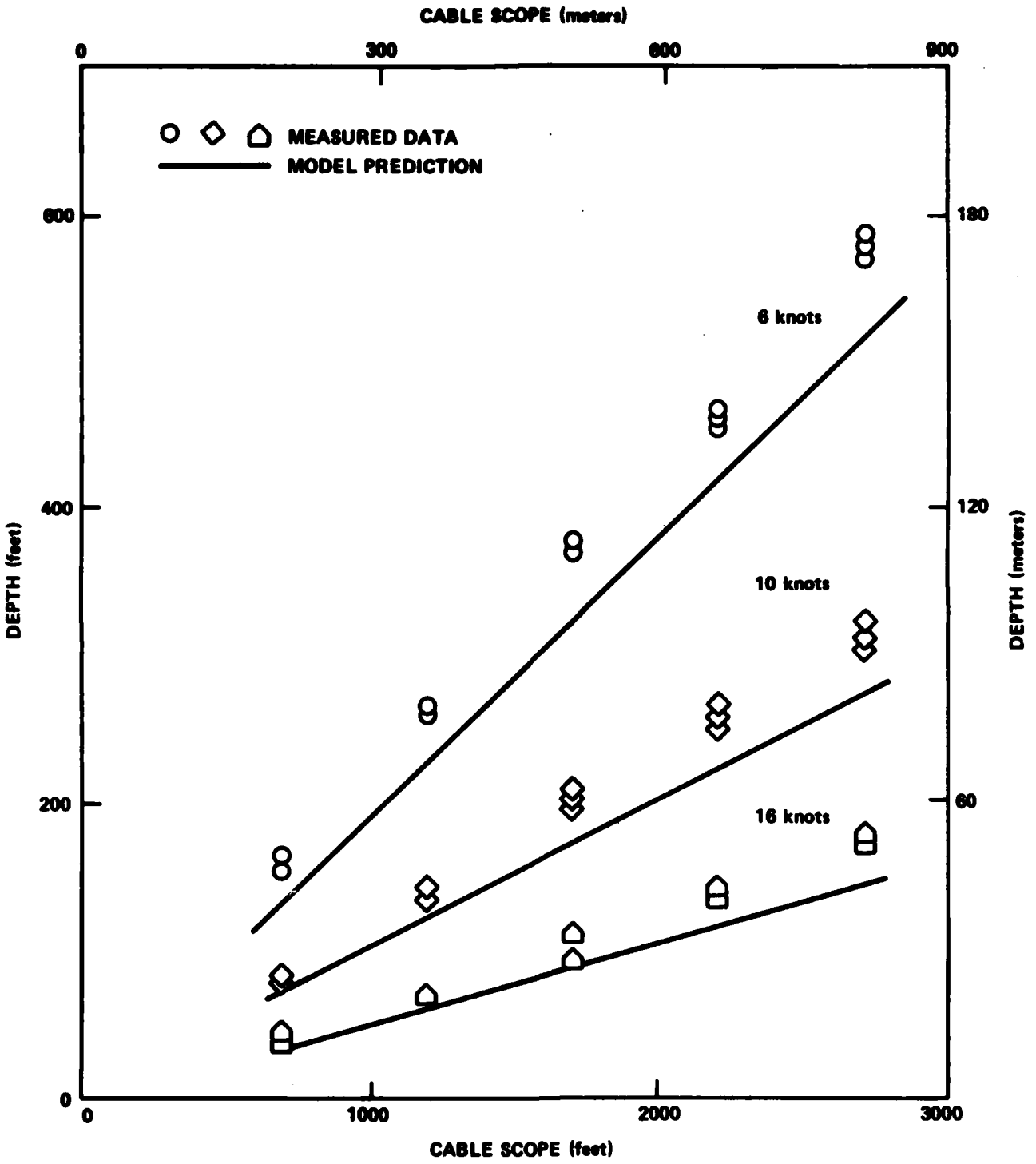

Figure 11 - Comparison of New Model Predictions and Measured Depth as a Function of Scope for 0.542-Inch (1.38-Centimeter) Diameter Towcable

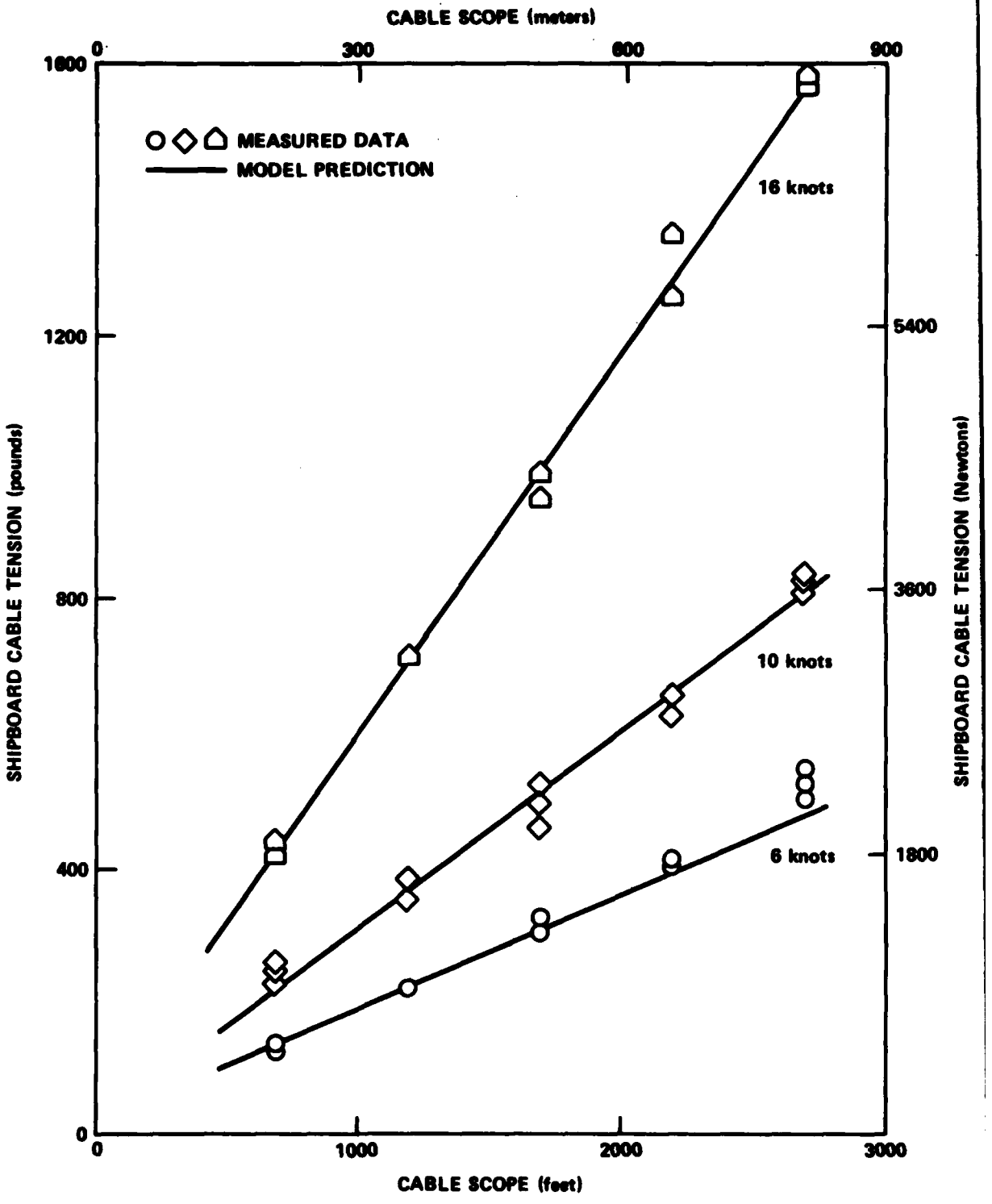

Figure 12 - Comparison of New Model Predictions and Measured Tension as a Function of Scope for 0.542-Inch (1.38-Centimeter) Diameter Towcable

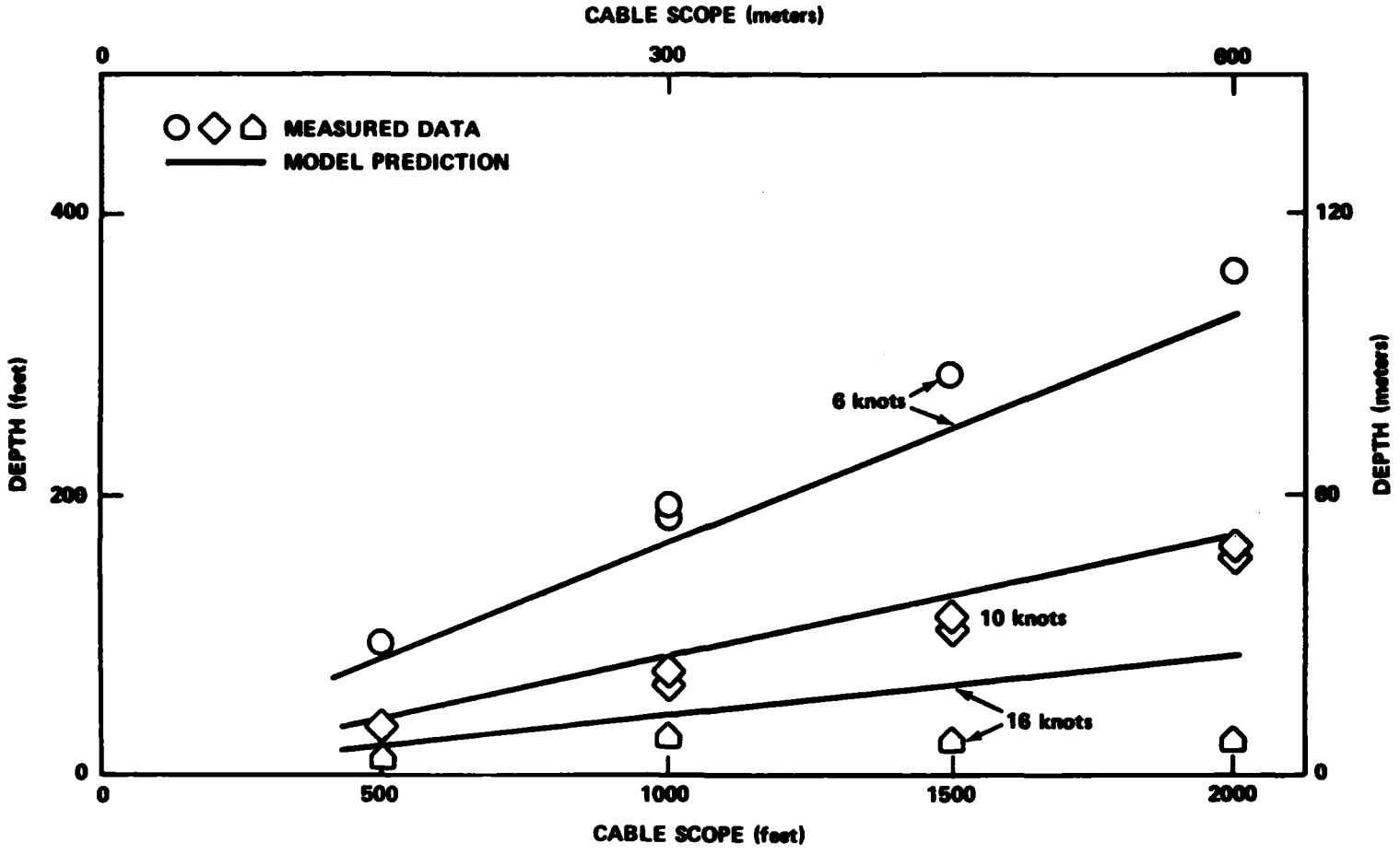

Figure 13 - Comparison of New Model Predictions and Measured Depth as a Function of Scope for 0.322-Inch (0.82-Centimeter) Diameter Towcable

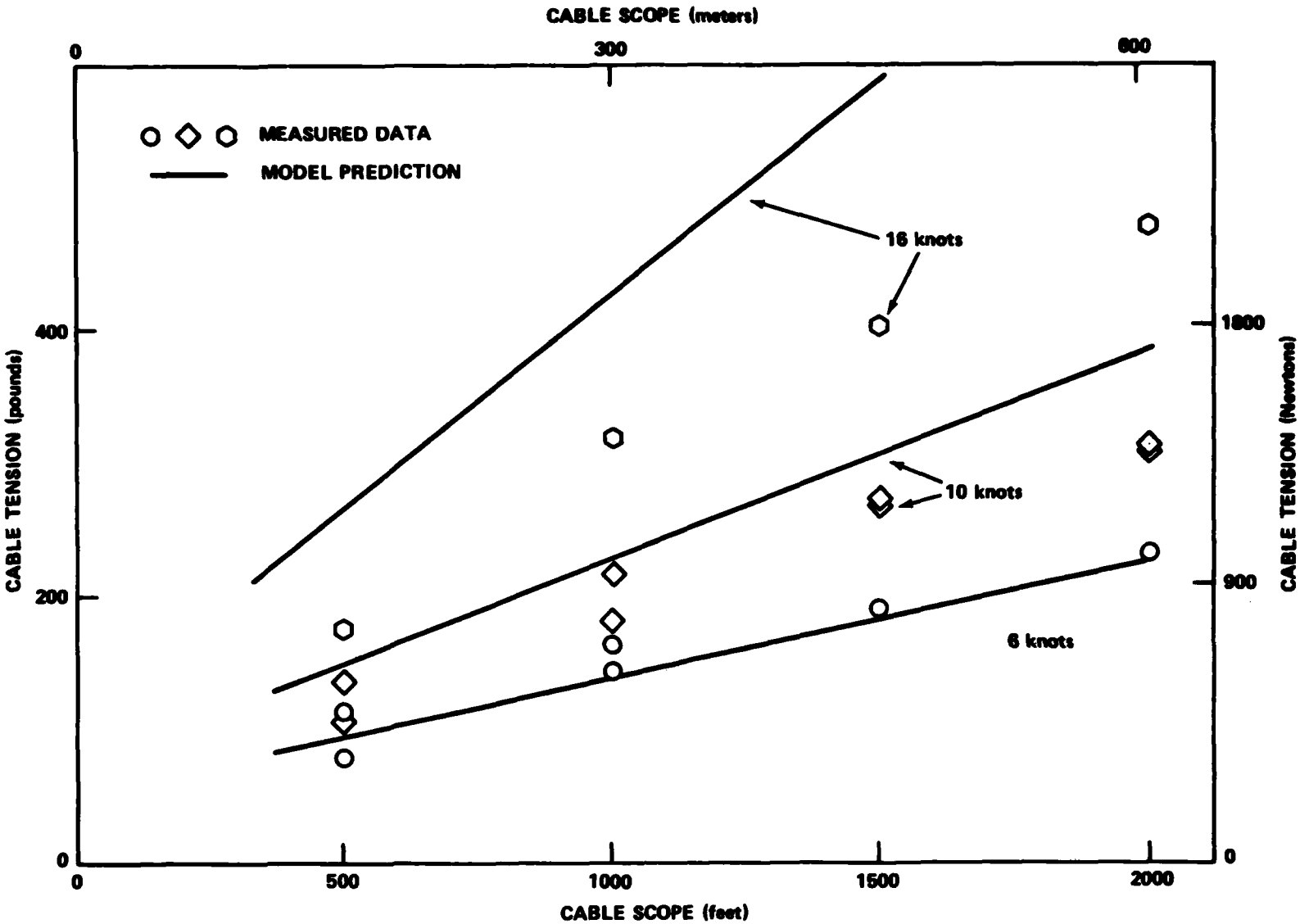

Figure 14 - Comparison of New Model Predictions and Measured Tension as a Function of Scope for 0.322-Inch (0.82-Centimeter) Diameter Towcable

base and even though the tension measurements were not used in formulating $f_t(\phi)$ and model/data agreement, therefore, should not be expected, the comparison is presented for completeness. As seen in Figures 13 and 14 the agreement is fair at the low speed but becomes increasingly poor with increasing speed.

Figure 15 shows the measured data points from sea trial 4H8 (Reference 10) on a 0.84-inch (2.13-cm) diameter armored cable. The solid line represents new computational model predictions. The agreement for both depth and tension is very close. For the tension predictions a zero scope tension value was obtained by extrapolating the measured data at each speed to zero scope. These zero scope tension values represent the drag of a towed array used in the experiments and therefore were used to represent the body force in the computer predictions.

Figures 16, 17 and 18 show data from an at-sea experiment[2] on a 0.35-inch (0.89-cm) diameter cable in a body-dominated configuration. As seen the agreement between the measured data and the new computational model is good.

Overall the agreement between model predictions based on the newly derived $f_n(\phi)$ and $f_t(\phi)$ and the available measured data is judged to be good. The advantage of these functions is that with a single value of C_R they provide a model which will support first order engineering estimates for bare armored cable towing configurations over a wide range of cable angles both shallow and steep. However, where towing depth and tension must be known very accurately, a situation most likely to attend long cables in high speed (shallow critical angle) tows, an observation by Relf and Powell[5] in 1917 relative to stranded cables, still applies, namely that it is best to test the particular cable.

Some caution should be exercised in using the computational model. First, although there is a sizeable experimental data base to support the formulation of the loading functions at the shallow angles, there are significantly less data at angles greater than 10^o. In particular, $f_t(\phi)$ at values of ϕ above 10^o is based solely on the Reference 2 data and the assumption that $f_t(\phi)$ is zero at $\phi = 90^o$.

Also, it should be noted that the model is derived from measurements on towing configurations, not on mooring configurations. Mooring generally implies a range of steeper cable angles and lower Reynolds numbers. Thus no statement can be made regarding the suitability of this model to the mooring case.

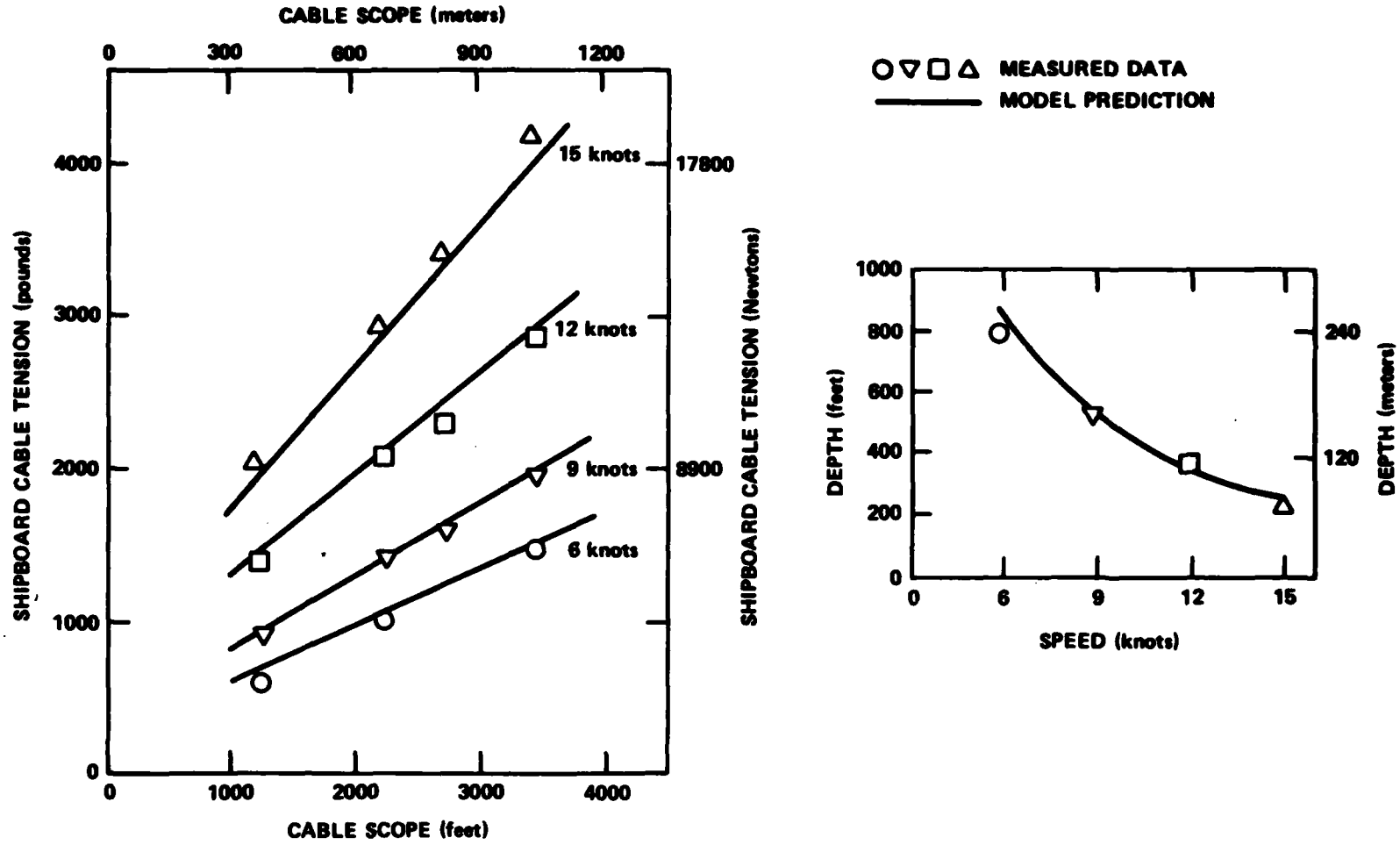

Figure 15 - Comparison of New Model Predictions and Measured Values of Tension and Depth from Sea Trial 4H8 for 0.84-Inch (2.13-Centimeter) Diameter Towcable

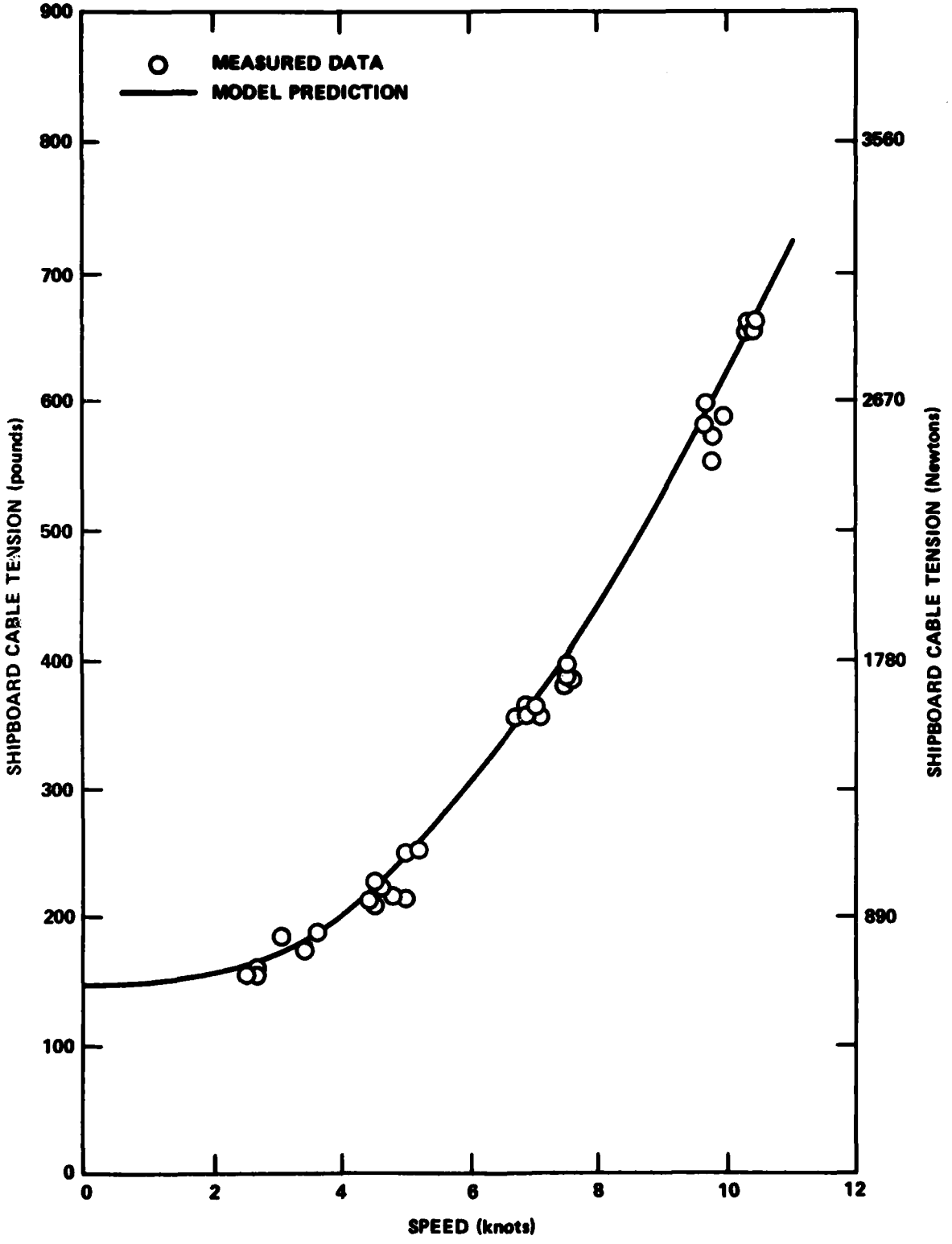

Figure 16 - Comparison of New Model Predictions and Measured Cable Tension for a Nominal Scope of 280 Feet (85.3 Meters)

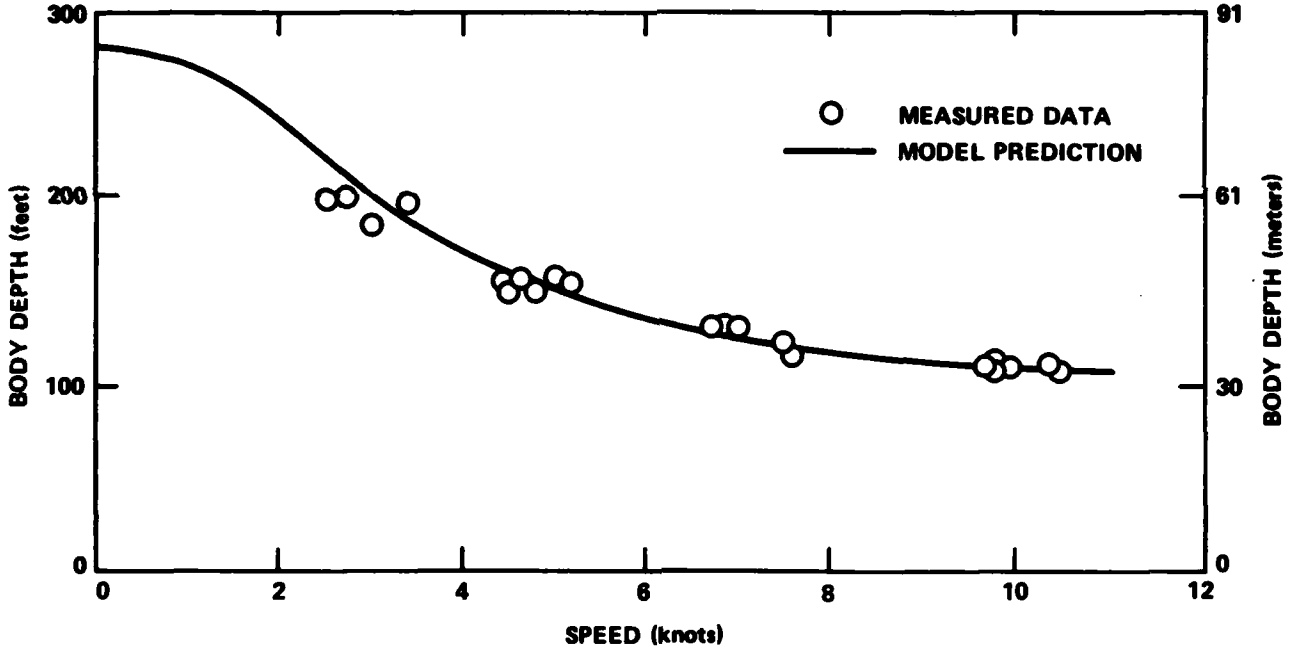

F ,ure 17 - Comparison of New Model Predictions and Measured Body Depth for a Nominal Cable Scope of 280 Feet (85.3 Meters)

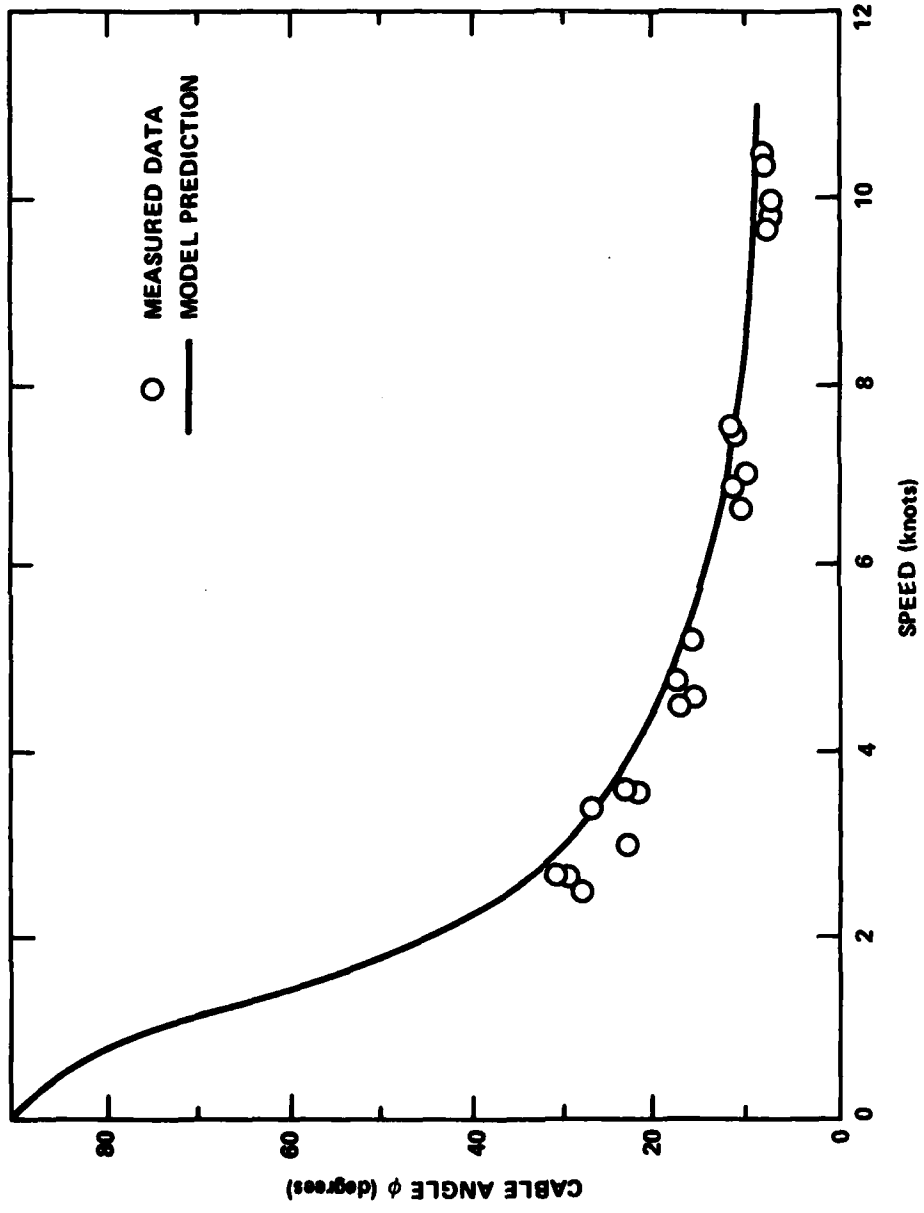

Figure 18 - Comparison of New Model Predictions and Measured Cable Angle at the Towing Ship for a Nominal Cable Scope of 280 Feet (85.3 Meters)

The fact that a single value of C_R independent of Reynolds number provides a good model fit to the data is surprising when considered in relation to the well known normal drag coefficient for a right circular cylinder (Figure 3). Somewhere in the R_n range covered by these experiments (Figure 4), it would be expected that transition with its marked reduction in C_R would occur. The free stream sees in reality a fine elliptical shape and a high degree of sweep to the span. Such factors of geometry would tend to diminish but not eliminate the R_n effects. It may be that R_n effects are masked because of the strong relationship which exists between R_n and ϕ over large portions of the measured data base (Figure 4).

The problem of model accuracy for the very shallow angle range is fundamental and from two sources. First there is the problem of making accurate measurements at sea at very shallow angles. The range of uncertainty in angle, wetted scope and velocity profile is relatively large. Second, both $f_n(\phi)$ and $f_t(\phi)$ are very sensitive to ϕ at shallow cable angles. This sensitivity is compounded in that an error in estimating ϕ (from $f_n(\phi)$) will magnify the error in predicting the tension ($f_t(\phi)$). With respect to the data bases used in this report, measurement accuracies cannot be quantified since this information was not provided in the source documents. In general, the accuracies are judged to have been as high as could be attained given the environmental limitations. For example, the towing basin provides very accurate control and measurement of speed and track but introduces artificialities in the restrictions depth places on cable length. The dynamics of the at-sea environment diminish the accuracies in all measurements.

The hydrodynamic loading function models need to be tested further against other independently acquired data bases. The reason for the data scatter, especially for $f_n(\phi)$ at shallow angles, needs to be determined; whether it is simply a problem in measurement accuracy or whether certain characteristics of the cable, not now explicitly treated here and influencing the data, needs to be ascertained. It should be noted that, while kiting has not been explicitly treated in this analysis, the loading functions have been developed with kiting implied. That is $f_n(\phi)$ and $f_t(\phi)$ have been developed from a data base of kiting towcables. Any predictions based on these loading functions will therefore pertain to kiting armored towcables. However, for a rigorous treatment of hydrodynamic loading kiting must be explicitly accounted for.

CONCLUSIONS

From the foregoing analysis it is concluded that:

1. Good first order engineering estimates of bare armored cable towing configurations over a broad range of cable angles for both critical angle tows and body-dominated tows can be obtained using $C_R = 1.5$ and a new set of hydrodynamic loading functions:

$$f_n(\phi) = 0.5 - 0.1\cos\phi + 0.1\sin\phi - 0.4\cos 2\phi - 0.011\sin 2\phi$$
$$f_t(\phi) = -0.1945 + 0.203\cos\phi + 0.1945\sin\phi - 0.0681\sin 2\phi$$

2. The fact that a constant value $C_R = 1.5$ provides a good fit to most of the data implies that R_n effects are not a significant factor in the hydrodynamics relative to this data base.

3. If critical angle towing configurations and tensions must be known very accurately, then the particular cable must be tested.

REFERENCES

1. Pode, L., "Tables for Computing the Equilibrium Configuration of a Flexible Cable in a Uniform Stream," David Taylor Model Basin Report 687 (Mar 1951).

2. Gibbons, T. and C. Walton, "Evaluation of Two Methods for Predicting Towline Tensions and Configurations of a Towed Body System Using Bare Cable," David Taylor Model Basin Report 2313 (Dec 1966).

3. Bishop, R. and A. Hassan, "The Lift and Drag Force on a Cylinder in a Flowing Fluid," Proceedings, Royal Society, London, Series A, Vol. 277 (1963) pp. 32-50.

4. Chiu, W. and J. Lienhard, "On Real Fluid Flow over Yawed Circular Cylinders," Journal of Basic Engineering (1967).

5. Relf, E. and C. Powell, "Tests on Smooth and Stranded Wires Inclined to the Wind Direction, and a Comparison of Results on Stranded Wires in Air and Water," British ARC, R&M 1917, Report 307.

6. Souders, W., D. Coder, and J. Nelka, "Experimental Measurements of Lift and Drag on an Oscillating, Smooth Circular Cylinder in Crossflow," NSRDC Report 302-H-01 (1968).

7. Coder, D., "Hydrodynamic Forces on Oscillating and Non-Oscillating Smooth Circular Cylinders in Crossflow," NSRDC Report 3639 (1972).

8. Blevins, R. and T. Burton, "Fluid Forces Induced by Vortex Shedding," ASME Publication 75-FE-10.

9. Ramsey, J. and D. Dillon, "Empirical Hydrodynamic Characteristics of Two Bare Double Armored Towlines," Hydrospace Research Corporation, Report 293 (Nov 1970).

10. Diggs, J., "Hydrodynamic Characterization of Various Towed Array Towcables," MAR, Inc., Technical Report 128 (Aug 1974).

11. Reid, R. and B. Wilson, "Boundary Flow Along a Circular Cylinder," National Engineering Science Co., Tech. Report 204-4 (Mar 1962).

12. Puryear, F. and S. Gay, "Hydrodynamic Loading of Six Configurations of a Towed Flexible Conduit," NSRDC Report 509-H-01 (Dec 1972).

INITIAL DISTRIBUTION

Copies

3 CNO
- 1 OP-224G
- 1 OP-353
- 1 OP-941B

4 CNR
- 1 ONR-220 (Gilmore)
- 1 ONR-230 (Naglehout)
- 1 ONR-260 (Siegel)
- 1 ONR-420 (Hamilton)

2 NRL
- 1 Code 5800
- 1 Code 7500 (W. Carey)

2 NAVMAT
- 1 PM-4
- 1 ASW-10

1 NAVAIR/Code 548

1 NADC

1 NADC/Key West

7 NELX
- 1 PME-106 (Kearney)
- 1 PME-107
- 1 PME-110
- 1 PME-124
- 1 PME-124-40
- 1 ELEX-06T (Lawson)
- 1 ELEX-3104

7 NAVSEA
- 1 SEA 05R
- 1 SEA 05X4
- 1 SEA 05L
- 1 SEA 61Z4
- 1 SEA 92
- 1 PMS-395
- 1 PMS-407

1 NCEL/Code L43 (D. Meggitt)

2 NCSC
- 1 Code 700 (Lacey)
- 1 Code 721-3 (Lloyd)

Copies

2 NOSC
- 1 Code 52 (Talkington)
- 1 Code 521 (LeMaire)

1 NSWC/Silver Spring, MD 20910/
Code D-23

1 NSWC/Dahlgren, VA 22448

1 NUSC/Fort Lauderdale, FL 33315
Code 3231 (Kennedy)

1 NUSC/Newport, RI 02840

3 NUSC/New London Laboratory
New London, CT 06320
- 1 Code 10
- 1 Code 201
- 1 Code 3343 (Rupinski)

1 NOAA
Engineering Support Office
P.O. Box 24079
Washington, D.C. 20024
(Kalvaitis)

12 DTIC

1 Applied Physics Laboratory
The Johns Hopkins University
Johns Hopkins Road
Laurel, MD 20707

1 Applied Physics Laboratory
The University of Washington
1013 N.E. 40th Street
Seattle, WA 98105
Dr. Dale Calkins

1 Applied Research Laboratory
Penn State University
P.O. Box 30
State College, PA 16801
Dr. Blaine Parkin

1 Applied Research Laboratory
The University of Texas at Austin
P.O. Box 8029
Austin, TX 78712

Copies

1 Defence Research Establishment
Atlantic/Dartmouth/Nova Scotia
Jim Tremills

1 Scripps Institution of
Oceanography/Marine Physical
Laboratory
La Jolla, CA 92093

1 Texas A&M University
Department of Oceanography
College Station, TX 77843
Dr. David R. Schink

1 Woods Hole Oceanographic Institute
Woods Hole, MA 02543

1 Applied Measurement Systems, Inc.
1415 S.W. 21st Avenue
Fort Lauderdale, FL 33312
Barry Douglass

1 Applied Measurement Systems, Inc.
P.O. Box 171
301 Flanders Road
E. Lyme, CT 06333
Jesse Diggs

1 Boeing Marine Systems
P.O. Box 3707
Seattle, WA 98124

1 Binary Systems, Inc.
88 Sunnyside Boulevard
Plainview, NY 11803
Dr. Sheldon Gardner

1 B-K Dynamics, Inc.
247 Shaw Street
New London, CT 06320
James Fitzgerald

1 Booz-Allen & Hamilton, Inc.
4330 East-West Highway
Bethesda, MD 20015

1 Boston Insulated Wire & Cable Co.
65 Ray Street
Boston, MA 02125
William Hill

Copies

1 Cortland Line Co.
67 E. Court Street
Cortland, NY 13045
Dr. E. Scala

1 Cross-Line Manufacturing Inc
Rt. 4, Box 2245
Navasota, TX 77868
Gary Griffin

1 Computer Sciences Corporatic
1616 N. Ft. Myer Drive
Arlington, VA 22209

1 Daedalean Associates, Inc.
Springlake Research Center
15110 Frederick Road
Woodbine, MD 21797

1 EDO Corporation
Fiber Science Division
506 Billy Mitchell Road
Salt Lake City, UT 84116

1 EG&G/WASC
2150 Fields Road
Rockville, MD 20850
Les Bonde

1 Epoch Engineering
2 Professional Drive
Suite 229
Gaithersburg, MD 20879
Martin Karchnak

1 Fathom Oceanology Ltd.
863 Rangeview Road
Port Credit
Ontario, Canada
Ken Gardner

1 Fleet Industries
P.O. Box 400
Gilmore Road
Fort Erie
Canada L2A 5N3
Al Perkins

Copies

1 General Electric Company
Farrell Road Plant
Building 1
Syracuse, NY 13201
Dr. Young Chey

1 General Offshore
7945 MacArthur Boulevard
Cabin John, MD 20731

1 General Offshore
2605 Stirling Road
Fort Lauderdale, FL 33312

1 Goodyear Aerospace Company
1210 Massillon Road
Akron, OH 44315

1 Gould, Inc.
Chesapeake Instrument Division
6711 Baymeadow Drive
Glen Burnie, MD 21061

1 Gulf Science and Technology Co.
P.O. Drawer 2038
Pittsburgh, PA 15230
Dr. R.J. Mousseau

1 Hydro Products
P.O. Box 2528
San Diego, CA 92112
Leon J. Corcoran

1 Interstate Electronics Corp.
1911 Jefferson Davis Highway
Suite 1001
Arlington, VA 22202
Dan Fryberger

1 James S. Krogen & Co., Inc.
3333 Rice Street
Miami, FL 33133
James S. Krogen

1 Lockheed Missile & Space Co., Inc.
Ocean Systems 0/57-24 B/568
1111 Lockheed Way
Sunnyvale, CA 94086
Herb Schreiber

Copies

1 MAR Associates, Inc.
1335 Rockville Pike
Rockville, MD 20852
Shelton Gay

1 MAR, Inc.
1335 Rockville Pike
Rockville, MD 20852
Roger Levin

1 MAR, Inc.
Marine Services Division
The Freeport Building
500 S.E. 24th Street
Fort Lauderdale, FL 33316
Al Yoder

1 MAR, Inc.
131 Boston Post Road
E. Lyme, CT 06333
Charles Veitch

1 MSM, Inc.
1 West Deer Park Road
Gaithersburg, MD 20879
Dr. Lewis Schneider

1 ORI
1400 Spring Street
Silver Spring, MD 20910
Don Berklew

1 K.G. Pollock & Associates
8240 Kings Arm Drive
Alexandria, VA 22308

1 Raytheon Company
P.O. Box 360
Portsmouth, RI 02871

1 The Rochester Corporation
Culpepper, VA 22701
Al Crane

1 Science Applications, Inc.
1710 Goodridge Drive
McLean, VA 22101

Copies

Copies	
1	Simplex Wire and Cable Co. 79 Sidney Street Cambridge, MA 02139
1	Spears Associates, Inc. 249 Vanderbilt Avenue Norwood, MA 02139
1	SRI, International Physical Sciences Division 333 Ravenswood Avenue Menlo Park, CA 94025 Dr. Sam Schechter
1	Telephonics Corporation 770 Park Avenue Huntington, NY 11743 Paul Hlesciak
1	Telephonics Corporation 5220C West Highway 98 Panama City, FL 32405 Jesse Duke
1	TRACOR 1601 Research Boulevard Rockville, MD 20850
1	TRACOR MARINE P.O. Box 13107 S.E. 19th Avenue at 35th Street Port Everglades, FL 33316
1	Vector Cable Company 555 Industrial Road Sugarland, TX 77478 H. Blumsack
1	Vector Research Company 6410 Rockledge Drive Bethesda, MD 20034
1	Westinghouse Electric Corp. Ocean Research & Engineering Center Box 1488 - MS 9105 Annapolis, MD 21404

CENTER DISTRIBUTION

Copies	Code	Name
1	1504	
1	1509	
1	152	
1	154	
2	1541	
1	156	
10	5211.1	Reports Distribution
1+1m	522.1	Unclassified Lib (C)
1	522.2	Unclassified Lib (A)

DTNSRDC ISSUES THREE TYPES OF REPORTS

1. DTNSRDC REPORTS, A FORMAL SERIES, CONTAIN INFORMATION OF PERMANENT TECHNICAL VALUE. THEY CARRY A CONSECUTIVE NUMERICAL IDENTIFICATION REGARDLESS OF THEIR CLASSIFICATION OR THE ORIGINATING DEPARTMENT.

2. DEPARTMENTAL REPORTS, A SEMIFORMAL SERIES, CONTAIN INFORMATION OF A PRELIMINARY, TEMPORARY, OR PROPRIETARY NATURE OR OF LIMITED INTEREST OR SIGNIFICANCE. THEY CARRY A DEPARTMENTAL ALPHANUMERICAL IDENTIFICATION.

3. TECHNICAL MEMORANDA, AN INFORMAL SERIES, CONTAIN TECHNICAL DOCUMENTATION OF LIMITED USE AND INTEREST. THEY ARE PRIMARILY WORKING PAPERS INTENDED FOR INTERNAL USE. THEY CARRY AN IDENTIFYING NUMBER WHICH INDICATES THEIR TYPE AND THE NUMERICAL CODE OF THE ORIGINATING DEPARTMENT. ANY DISTRIBUTION OUTSIDE DTNSRDC MUST BE APPROVED BY THE HEAD OF THE ORIGINATING DEPARTMENT ON A CASE-BY-CASE BASIS.